THE EUROPEAN
PHYSICAL JOURNAL C

CrossMark

Heavy neutrino mixing in the T2HK, the T2HKK and an extension of the T2HK with a detector at Oki Islands

Yugo Abe[1,2], **Yusuke Asano**[1], **Naoyuki Haba**[1], **Toshifumi Yamada**[1,a]

[1] Graduate School of Science and Engineering, Shimane University, Matsue 690-8504, Japan
[2] National Institute of Technology, Miyakonojo College, Miyakonojo-shi Miyazaki 885-8567, Japan

Abstract We study the discovery potential for the mixing of heavy isospin-singlet neutrinos in extensions of the Tokai-to-Kamioka (T2K) experiment, the Tokai-to-Hyper-Kamiokande (T2HK), the Tokai-to-Hyper-Kamiokande-to-Korea (T2HKK) with a Korea detector with $\simeq 1000$ km baseline length and $1°$ off-axis angle, and a plan of adding a small detector at Oki Islands to the T2HK. We further pursue the possibility of measuring the neutrino mass hierarchy and the standard CP-violating phase δ_{CP} in the presence of heavy neutrino mixing by fitting data with the standard oscillation parameters only. We show that the sensitivity to heavy neutrino mixing is highly dependent on δ_{CP} and new CP-violating phases in the heavy neutrino mixing matrix, and deteriorates considerably when these phases conspire to suppress interference between the standard oscillation amplitude and an amplitude arising from heavy neutrino mixing, at the first oscillation peak. Although this suppression is avoided by the use of a beam with smaller off-axis angle, the T2HKK and the T2HK+small Oki detector do not show improvement over the T2HK. As for the mass hierarchy measurement, the wrong mass hierarchy is possibly favored in the T2HK because heavy neutrino mixing can mimic matter effects. In contrast, the T2HKK and the T2HK+small Oki detector are capable of correctly measuring the mass hierarchy despite heavy neutrino mixing, as measurements with different baselines resolve degeneracy between heavy neutrino mixing and matter effects. Notably, adding a small detector at Oki to the T2HK drastically ameliorates the sensitivity, which is the central appeal of this paper. As for the δ_{CP} measurement, there can be a sizable discrepancy between the true δ_{CP} and the value obtained by fitting data with the standard oscillation parameters only, which can be comparable to 1σ resolution

of the δ_{CP} measurement. Hence, if a hint of heavy neutrino mixing is discovered, it is necessary to incorporate the effects of heavy neutrino mixing to measure δ_{CP} correctly.

1 Introduction

It is a viable possibility that isospin-singlet neutrinos mix with active flavors ν_e, ν_μ, ν_τ after electroweak symmetry breaking. Notably, such a mixing is inherent in the Type-I seesaw model [1–4], and although the mixing angle is undetectably small in most of the parameter space, it can be sizable when there is a cancellation in the seesaw mass. To see this, suppose, for example, there are three isospin-singlet neutrinos with a Majorana mass M_N, having a Dirac mass term m_D with active neutrinos. Since the tiny neutrino mass is derived as $-m_D M_N^{-1} m_D^T$, one can express m_D as [5]

$$m_D = U_{PMNS}\, i \begin{pmatrix} \sqrt{m_1} & 0 & 0 \\ 0 & \sqrt{m_2} & 0 \\ 0 & 0 & \sqrt{m_3} \end{pmatrix} R_3(\alpha, \beta, \gamma)\, \sqrt{M_N},$$

(1)

where U_{PMNS} denotes the Pontecorvo–Maki–Nakagawa–Sakata (PMNS) mixing matrix [6–8], m_1, m_2, m_3 are the tiny neutrino mass, and R_3 is a 3-dimensional rotation matrix with complex-valued rotation angles α, β, γ. Unless m_1, m_2, m_3 are degenerate, one can arbitrarily enhance m_D and the mixing angles between isospin-singlet and active neutrinos by taking large imaginary values for α, β, γ. In this case, a cancellation is taking place in the components of $-m_D^T M_N^{-1} m_D$. Large mixing between isospin-singlet and active neutrinos is also realized in extensions of the Type-I seesaw model, such as the inverse seesaw model [9,10].

In the presence of isospin-singlet neutrino mixing, transitions among active flavors require for their consistent description extra parameters beyond the standard oscillation param-

Springer

eters, the three mixing angles θ_{12}, θ_{23}, θ_{13}, one CP-violating phase δ_{CP} and two mass differences Δm_{12}^2, Δm_{13}^2. Tension in fitting neutrino oscillation data with the standard parameters would thus be evidence for isospin-singlet neutrino mixing. If isospin-singlet neutrinos are "heavy", by which we mean that their mass is much above the neutrino beam energy, they do not contribute to oscillations and simply alter the mixing matrix U_{PMNS} into a non-unitary matrix in the following fashion:

$$U_{PMNS} \rightarrow \begin{pmatrix} \alpha_{11} & 0 & 0 \\ \alpha_{21} & \alpha_{22} & 0 \\ \alpha_{31} & \alpha_{32} & \alpha_{33} \end{pmatrix} U_{PMNS} \tag{2}$$

where α_{ii}'s are real and α_{ij}'s ($i \neq j$) are complex numbers.

One purpose of this paper is to estimate the largest possible significance of heavy isospin-singlet neutrino mixing in the Tokai-to-Hyper-Kamiokande (T2HK) [11] and the Tokai-to-Hyper-Kamiokande-to-Korea (T2HKK) [12] (for early proposals, see Refs. [13–23]) experiments, as well as an experiment in which a new detector at Oki Islands is added to the T2HK (for early proposals on a detector at Oki, see Refs. [22–24]). Emphasis is on how the significance varies with CP-violating phases in the PMNS and the non-unitary mixing matrices and to what extent the sensitivity deteriorates with these phases. The secondary goal of this paper is to pursue the possibility that the neutrino mass hierarchy and the standard CP-violating phase in the PMNS matrix δ_{CP} are measured in the presence of heavy neutrino mixing by fitting neutrino data with the standard oscillation parameters only, namely, without assuming heavy neutrino mixing. This is achievable if data allow us to discern contributions from the standard oscillation and those from the non-unitary mixing matrix. Such measurement is of practical importance when a hint of heavy neutrino mixing were discovered but were not conclusive. The mass hierarchy and δ_{CP} measurement in the presence of heavy neutrino mixing has been investigated in a general context [25] and for the T2K, T2HK, NOνA and DUNE experiments [26–29].

The T2HK and the T2HKK are proposed extensions of the on-going T2K experiment [31], utilizing an off-axis $\nu_\mu + \bar{\nu}_\mu$ beam delivered from J-PARC. In the T2HK, there are two water Cerenkov detectors, each with 187 kton fiducial volume, located solely at Kamioka, where the baseline length is $L = 295$ km and the off-axis-angle is $2.5°$. In one plan of the T2HKK, one water Cerenkov detector with 187 kton fiducial volume is placed at Kamioka and the same detector is also at a site in Korea where the baseline length is $L \simeq 1000$ km and the off-axis-angle is $1°$. We also consider a plan of placing, in addition to the T2HK, a small 10 kton water Cerenkov detector at Oki Islands, where the baseline length is $L = 653$ km and the off-axis-angle is $1.0°$.

The merits of the above long baseline experiments for the search for heavy neutrino mixing are as follows: (i) In disappearance experiments, the effects of heavy neutrino mixing as parametrized by Eq. (2) cancel between measurements at the near and far detectors, while the T2K and its extensions are primarily appearance experiments. (ii) $\nu_\mu \rightarrow \nu_e$ ($\bar{\nu}_\mu \rightarrow \bar{\nu}_e$) transition amplitude arising from the non-unitary mixing matrix Eq. (2) interferes with the standard oscillation amplitude, enhancing the impact of non-unitary mixing on the transition probability. The merit (ii), however, bears two subtleties:

- CP-violating phases in the PMNS and the non-unitary mixing matrices possibly lead to suppression of the interference.
- Non-unitary mixing α_{21} in Eq. (2) can mimic matter effects and the effect of the standard phase δ_{CP}, which distorts the measurement of the mass hierarchy and δ_{CP}.

These issues become transparent by expressing the transition amplitude in the leading order of $\sin\theta_{13}$, Δm_{21}^2, α_{21} and matter effects as

$$
\begin{aligned}
i\langle \nu_e | e^{-i\int_0^L dx\, H(x)} | \nu_\mu \rangle &= 2\, e^{-i\Delta m_{31}^2 L/(4E)} \\
&\times \sin\left(\frac{\Delta m_{31}^2 L}{4E}\right) e^{-i\delta_{CP}} \sin\theta_{13} \sin\theta_{23} \\
&+ \frac{\Delta m_{21}^2 L}{4E} \sin(2\theta_{12}) \cos\theta_{23} + i\alpha_{21}^* \\
&- i V_{cc} L \left\{ \frac{\Delta m_{31}^2 L}{4E} e^{-i\delta_{CP}} \sin\theta_{13} \sin\theta_{23} \right. \\
&\left. + \frac{1}{2}\frac{\Delta m_{21}^2 L}{4E} \sin(2\theta_{12}) \cos\theta_{23} \right\},
\end{aligned}
\tag{3}
$$

$$
\begin{aligned}
i\langle \bar{\nu}_e | e^{-i\int_0^L dx\, H(x)} | \bar{\nu}_\mu \rangle &= 2\, e^{-i\Delta m_{31}^2 L/(4E)} \\
&\times \sin\left(\frac{\Delta m_{31}^2 L}{4E}\right) e^{i\delta_{CP}} \sin\theta_{13} \sin\theta_{23} \\
&+ \frac{\Delta m_{21}^2 L}{4E} \sin(2\theta_{12}) \cos\theta_{23} + i\alpha_{21} \\
&+ i V_{cc} L \left\{ \frac{\Delta m_{31}^2 L}{4E} e^{i\delta_{CP}} \sin\theta_{13} \sin\theta_{23} \right. \\
&\left. + \frac{1}{2}\frac{\Delta m_{21}^2 L}{4E} \sin(2\theta_{12}) \cos\theta_{23} \right\},
\end{aligned}
\tag{4}
$$

where E denotes the neutrino energy and L the baseline length, and V_{cc} is the potential due to charged current interaction inside matter.

We notice that the following interference terms:

$$|\langle \nu_e| e^{-i \int_0^L dx\, H(x)} |\nu_\mu\rangle|^2$$
$$\supset -4 \sin\left(\frac{\Delta m_{31}^2 L}{4E}\right) \sin\theta_{13} \sin\theta_{23}$$
$$\times \operatorname{Im}\left(\alpha_{21} e^{-i\Delta m_{31}^2 L/(4E) - i\delta_{CP}}\right)$$
$$+ 2\frac{\Delta m_{21}^2 L}{4E} \sin(2\theta_{12}) \cos\theta_{23} \operatorname{Im}(\alpha_{21}), \qquad (5)$$

$$|\langle \bar\nu_e| e^{-i \int_0^L dx\, H(x)} |\bar\nu_\mu\rangle|^2$$
$$\supset 4 \sin\left(\frac{\Delta m_{31}^2 L}{4E}\right) \sin\theta_{13} \sin\theta_{23}$$
$$\times \operatorname{Im}\left(\alpha_{21} e^{i\Delta m_{31}^2 L/(4E) - i\delta_{CP}}\right)$$
$$- 2\frac{\Delta m_{21}^2 L}{4E} \sin(2\theta_{12}) \cos\theta_{23} \operatorname{Im}(\alpha_{21}), \qquad (6)$$

are simultaneously suppressed at the first oscillation peak, $\Delta m_{31}^2 L/(4E) = \pi/2$, if $\operatorname{Arg}(\alpha_{21}) \simeq \delta_{CP} \pm \pi/2$ holds accidentally (note the relation $\Delta m_{21}^2 L/(4E) \simeq 0.1 \cdot 2 \sin\theta_{13}$ at the first oscillation peak). This suppression is mitigated if the energy distribution is not concentrated at the first oscillation peak. We thus infer that when $\operatorname{Arg}(\alpha_{21}) \simeq \delta_{CP} \pm \pi/2$ holds, the T2HKK with a Korea detector placed at 1° off-axis angle exhibits better sensitivity to α_{21} than the T2HK, and that the extension of the T2HK with an Oki detector gives qualitative improvement. Of course, these anticipations depend on statistics, namely, competition with the loss of statistics in the T2HKK, or the size of an Oki detector.

We observe in Eqs. (3) and (4) that when $\delta_{CP} \simeq 0, \pi$, the real part of non-unitary mixing $\operatorname{Re}(\alpha_{21})$ plays exactly the same role as matter effects, which afflicts the measurement of the mass hierarchy because it is probed through interference with matter effects. However, when measurements with different baselines and hence different $V_{cc}L$'s are combined, one resolves degeneracy between the non-unitary mixing and matter effects, thereby resurrecting sensitivity to the mass hierarchy. We thus expect that the mass hierarchy measurement in the T2HK is subject to strong influence from heavy neutrino mixing, whereas the T2HKK maintains sensitivity to the mass hierarchy even with heavy neutrino mixing. Also, the addition of a small detector at Oki to the T2HK leads to qualitative improvement in the mass hierarchy measurement.

Equations (3), (4) tell us that when $\delta_{CP} \simeq \operatorname{Arg}(\alpha_{21})$, non-unitary mixing α_{21} and the first term in the first line of Eqs. (3) and (4), which is proportional to $e^{i\delta_{CP}}$, interfere maximally. In such a case, the presence of α_{21} affects the measurement of δ_{CP} and causes a discrepancy between the true δ_{CP} and the value measured by fitting data with the standard oscilla-

tion parameters only. This effect is mitigated if the baseline is longer, because more information as regards the energy dependence of the standard oscillation amplitude helps distinguish it from non-unitary mixing α_{21}. We thus expect that the discrepancy is smaller in the T2HKK than in the T2HK.

In the main body of this paper, we demonstrate, through a simulation, the following:

(a) The sensitivity to heavy neutrino mixing is suppressed for $\operatorname{Arg}(\alpha_{21}) \simeq \delta_{CP} \pm \pi/2$. Contrary to our anticipations, the T2HK shows better sensitivity than the T2HKK for any values of CP-violating phases, simply because of higher statistics. Also, adding a small detector at Oki to the T2HK does not make qualitative difference.

(b) In the presence of heavy neutrino mixing, the wrong mass hierarchy can be favored in the T2HK. The T2HKK maintains sensitivity to the mass hierarchy and measures it correctly despite heavy neutrino mixing. The extension of the T2HK with a small detector at Oki exhibits revived sensitivity to the mass hierarchy, even if statistics at Oki is quite subdominant compared to that at Kamioka.

(c) In the presence of heavy neutrino mixing, the true δ_{CP} and the value obtained by fitting data with the standard oscillation parameters can have a discrepancy which is of the same order as 1σ resolution of the δ_{CP} measurement. The discrepancy tends to be larger in the T2HK than in the T2HKK. Adding a small Oki detector to the T2HK does not make any difference.

Our most prominent finding is related to (b), which is that adding a small 10 kton detector at Oki to the T2HK leads to revived sensitivity to the mass hierarchy.

This paper is organized as follows: In Sect. 2, we present the formalism for incorporating the effects of heavy isospin-singlet neutrino mixing with a non-unitary mixing matrix. In Sect. 3, we estimate the largest possible significance of heavy neutrino mixing in the T2HK, the T2HKK and the extension of the T2HK with a small detector at OKi, and we further study the mass hierarchy and δ_{CP} measurement in the presence of heavy neutrino mixing. Here, we describe our benchmark model, procedures for simulating the long baseline experiments, and analysis with a χ^2 fitting. Sect. 4 summarizes the paper.

2 Formalism for incorporating heavy isospin-singlet neutrino mixing

Suppose we have $N - 3$ isospin-singlet neutrinos ν_{s_f} ($f = 4, 5, \ldots, N$) in addition to the three active flavors ν_e, ν_μ, ν_τ. Accordingly, there are N mass eigenstates ν_i ($i = 1, 2, \ldots, N$) belonging to mass eigenvalues m_i^2 and the neutrino mixing is expressed as

$$|\nu_\alpha\rangle = \sum_{i=1}^{N} U_{\alpha i} |\nu_i\rangle, \quad \alpha = e, \mu, \tau, s_f, \tag{7}$$

where $U_{\alpha i}$ is a $N \times N$ unitary matrix. In this paper, the $N - 3$ isospin-singlet neutrinos are assumed to be heavier than about 10 GeV.

In long baseline neutrino oscillation experiments, only the light mass eigenstates ν_1, ν_2, ν_3 are produced and propagate. Therefore, the probability for a neutrino of active flavor α with energy E to transition to active flavor β after traveling a distance L inside matter is

$$P(\nu_\alpha \to \nu_\beta) = \left| \langle \nu_\beta | U_{3\times3} \exp\left(-i \int_0^L dx\, H(x)\right) (U^\dagger)_{3\times3} |\nu_\alpha\rangle \right|^2$$
$$\times \ (\alpha, \beta = e, \mu, \tau), \tag{8}$$

$$H(x) = \text{diag}\left(-\sqrt{E^2 - m_1^2}, -\sqrt{E^2 - m_2^2}, -\sqrt{E^2 - m_3^2}\right) \tag{9}$$

$$+ \left[U^\dagger \text{diag}\,(\,V_{nc}(x) + V_{cc}(x),\ V_{nc}(x), \right.$$
$$\left. \times \ V_{nc}(x),\ 0, \ldots, 0\,)\, U \right]_{3\times3}, \tag{10}$$

where $U_{3\times3}$ denotes the $\alpha = e, \mu, \tau$ and $i = 1, 2, 3$ part of the mixing matrix U in Eq. (7), and $(U^\dagger)_{3\times3}$ denotes the same part for $U^\dagger$. Note that $U_{3\times3} \neq (U^\dagger)_{3\times3}$ in general. The factor $-\sqrt{E^2 - m_i^2}$ $(i = 1, 2, 3)$ is derived from the fact that a phase shift due to time evolution, $E\,dt$, is equivalent to $-\sqrt{E^2 - m_i^2}\,dx$ for the mass eigenstate with mass m_i. $[\ldots]_{3\times3}$ in Eq. (10) signifies that one extracts the $i, j = 1, 2, 3$ part of the $N \times N$ matrix. $V_{nc}(x)$ is the potential of the neutral current interaction inside matter divided by the neutrino velocity, and $V_{cc}(x)$ is that of the charged current interaction, which are evaluated to be

$$V_{nc}(x)\, L = -\frac{1}{\sqrt{2}} G_F n_n$$
$$L = -Y_n\, 0.193 \left(\frac{\rho(x)}{\text{g/cm}^3}\right) \left(\frac{L}{1000\ \text{km}}\right),$$
$$V_{cc}(x)\, L = \sqrt{2} G_F n_e$$
$$L = Y_e\, 0.385 \left(\frac{\rho(x)}{\text{g/cm}^3}\right) \left(\frac{L}{1000\ \text{km}}\right), \tag{11}$$

where n_n and n_e, respectively, denote the neutron and electron number density, Y_n and Y_e are, respectively, the number of neutrons and electrons per one nucleon, which are typically 1/2, and $\rho(x)$ is the matter density.

It is convenient to parametrize U in terms of mixing angles, θ_{ij}, and CP-violating phases, ϕ_{ij}, $(i < j, i, j = 1, 2, \ldots, N)$[1] as [30,33] (for the case with $N = 6$, see also Refs. [34,35])

---

[1] Only $(N-1)(N-2)/2$ linear combinations out of $N(N-1)/2$ phases ϕ_{ij}'s are physical.

$$U = \Omega_{N-1,N}\, \Omega_{N-2,N} \cdots \Omega_{1,N}\, \Omega_{N-2,N-1}\, \Omega_{N-3,N-1}$$
$$\cdots \Omega_{1,N-1}\, \Omega_{N-3,N-2} \cdots \Omega_{1,2},$$
$$(\Omega_{n,m})_{kk} = 1 \ \text{for} \ k \neq n, m,$$
$$(\Omega_{n,m})_{nn} = (\Omega_{n,m})_{mm} = \cos\theta_{nm},$$
$$(\Omega_{n,m})_{nm} = \sin\theta_{nm}\, e^{-i\phi_{nm}},$$
$$(\Omega_{n,m})_{mn} = -\sin\theta_{nm}\, e^{i\phi_{nm}}, \quad (\Omega_{n,m})_{kl} = 0 \ \text{otherwise.} \tag{12}$$

Note that the PMNS mixing matrix U_{PMNS} corresponds to $(\Omega_{2,3}\Omega_{1,3}\Omega_{1,2})$ with phases ϕ_{12}, ϕ_{23} set to 0 by the phase redefinition of $|\nu_1\rangle$, $|\nu_2\rangle$. We can thus express U in terms of the PMNS mixing matrix as

$$U = \begin{pmatrix} N_{NU} U_{PMNS} & S_{3\times N-3} \\ W_{N-3\times3} & T_{N-3\times N-3} \end{pmatrix},$$
$$N_{NU} = \begin{pmatrix} \alpha_{11} & 0 & 0 \\ \alpha_{21} & \alpha_{22} & 0 \\ \alpha_{31} & \alpha_{32} & \alpha_{33} \end{pmatrix}, \tag{13}$$

where $S_{3\times N-3}$, $W_{N-3\times3}$ and $T_{N-3\times N-3}$ denote $3 \times (N-3)$, $(N-3) \times 3$ and $(N-3) \times (N-3)$ matrices, respectively, α_{11}, α_{22} and α_{33} are real numbers and α_{21}, α_{31} and α_{32} are complex ones.

Since the mixing between isospin-singlet and active neutrinos is already constrained to be tiny, we make the approximation that we ignore terms in the second order of the mixing angles between active and isospin-singlet neutrinos. This gives $(U^\dagger)_{3\times3} = (U_{3\times3})^\dagger$ and

$$\left[U^\dagger \text{diag}\,(\,V_{nc}(x) + V_{cc}(x),\ V_{nc}(x),\ V_{nc}(x),\ 0, \ldots, 0\,)\, U \right]_{3\times3}$$
$$= (U_{3\times3})^\dagger\, \text{diag}\,(\,V_{nc}(x) + V_{cc}(x),\ V_{nc}(x),\ V_{nc}(x)\,)\, U_{3\times3}\,.$$

We then arrive at the following formula for the transition probabilities:

$$P(\nu_\alpha \to \nu_\beta) = \left| \langle \nu_\beta | N_{NU} U_{PMNS} \exp\left(-i \int_0^L dx\, H(x)\right) \right.$$
$$\left. \times\, U^\dagger_{PMNS} N^\dagger_{NU} |\nu_\alpha\rangle \right|^2 (\alpha, \beta = e, \mu, \tau),$$
$$H(x) = \frac{1}{2E} \text{diag}\left(0,\ \Delta m_{21}^2,\ \Delta m_{31}^2\right) + U^\dagger_{PMNS} N^\dagger_{NU}$$
$$\times \begin{pmatrix} V_{nc}(x) + V_{cc}(x) & 0 & 0 \\ 0 & V_{nc}(x) & 0 \\ 0 & 0 & V_{nc}(x) \end{pmatrix}$$
$$\times\, N_{NU} U_{PMNS}, \tag{14}$$

where we have made a further approximation with $E^2 \gg m_1^2, m_2^2, m_3^2$ and discarded terms proportional to the unit matrix in $H(x)$. The transition probabilities for antineutrinos, $P(\bar\nu_\alpha \to \bar\nu_\beta)$, are obtained by changing $\delta_{CP} \to -\delta_{CP}$ in U_{PMNS}, $\alpha_{ij} \to \alpha^*_{ij}$ in N_{NU}, and $V_{cc}(x) \to -V_{cc}(x)$, $V_{nc}(x) \to -V_{nc}(x)$ in Eq. (14).

3 Significance of heavy neutrino mixing and its effects on the mass hierarchy and δ_{CP} measurement

We estimate the largest possible significance of heavy neutrino mixing and its effects on the mass hierarchy and δ_{CP} measurement, through the following simulation: first we introduce a benchmark model where α_{11}, α_{22}, $|\alpha_{21}|$ in Eq. (2) are set at the current experimental bounds, in order to evaluate maximal impact of heavy neutrino mixing. Neutrino detection in the T2HK, the T2HKK, and the extension of the T2HK with a small detector at Oki is simulated based on the above benchmark, with Particle Data Group values employed for the standard parameters θ_{12}, θ_{23}, θ_{13}, Δm_{21}^2, $|\Delta m_{31}^2|$. Since no conclusive data on the mass hierarchy and δ_{CP} exist, and the phase of α_{21} is undetermined in the benchmark, we repeat the simulation for both mass hierarchies and for various values of δ_{CP} and $\text{Arg}(\alpha_{21})$. To assess merits of the extension of the T2HK with an Oki detector, we additionally consider, for comparative study, an experiment where the detector at Oki is instead placed at Kamioka. Finally, we perform a χ^2 fit of the simulation results under the assumption that no heavy neutrino mixing is present, namely, $N_{NU} = I_3$ in Eq. (13). The minimum of χ^2 is the square of the significance of heavy neutrino mixing. The mass hierarchy and the value of δ_{CP} with which χ^2 is minimized correspond to their measured values obtained without assuming heavy neutrino mixing.

3.1 Benchmark model

Our analysis is based on the following benchmark model: We employ the parametrization of Eq. (13). Since $\nu_\mu \to \nu_e$ process is most affected by α_{11}, α_{22} and α_{21}, we further set

$$N_{NU} = \begin{pmatrix} \alpha_{11} & 0 & 0 \\ \alpha_{21} & \alpha_{22} & 0 \\ 0 & 0 & 1 \end{pmatrix}. \qquad (15)$$

At present, the most severe constraint on α_{11}, α_{22} and α_{21} derives from experimental tests of lepton flavor universality and a mathematical inequality among α_{11}, α_{22} and α_{21}. These are enumerated below:

- One test of lepton flavor universality has been done in $\pi^\pm$ decays. When the non-unitary matrix Eq. (15) enters into the neutrino mixing Eq. (7), the ratio of the branching fractions becomes

$$\frac{\Gamma(\pi^\pm \to e^\pm \nu)}{\Gamma(\pi^\pm \to \mu^\pm \nu)} = \frac{m_e^2}{m_\mu^2} \frac{\left(1 - m_e^2/m_{\pi^\pm}^2\right)^2}{\left(1 - m_\mu^2/m_{\pi^\pm}^2\right)^2}$$
$$\times (1 + \epsilon_{SM}) \frac{\alpha_{11}^2}{\alpha_{22}^2 + |\alpha_{21}|^2}, \qquad (16)$$

where ϵ_{SM} indicates a Standard Model correction taking into account final state radiation. The experimental value and the Standard Model prediction are, respectively, given by [36–38,42,43]

$$\frac{\Gamma(\pi^\pm \to e^\pm \nu)}{\Gamma(\pi^\pm \to \mu^\pm \nu)}|_{\text{experimental}}$$
$$= (1.2354 \pm 0.0002) \times 10^{-4},$$
$$\frac{m_e^2}{m_\mu^2} \frac{\left(1 - m_e^2/m_{\pi^\pm}^2\right)^2}{\left(1 - m_\mu^2/m_{\pi^\pm}^2\right)^2}(1 + \epsilon_{SM})$$
$$= (1.230 \pm 0.004) \times 10^{-4}, \qquad (17)$$

from which we obtain the following bound:

$$\frac{\alpha_{11}^2}{\alpha_{22}^2 + |\alpha_{21}|^2} = 0.9956 \pm 0.0032. \qquad (18)$$

- Another test of lepton flavor universality comes from unitarity test of the Cabibbo–Kobayashi–Maskawa (CKM) matrix. In the presence of the non-unitary matrix Eq. (15), the Fermi constant measured in the muon decay becomes $G_\mu = G_F \alpha_{11} \sqrt{\alpha_{22}^2 + |\alpha_{21}|^2}$, whereas the Fermi constant measured in decays of hadrons involving $e\nu$ becomes $G_\beta = G_F \alpha_{11}$. Deviation of G_β/G_μ from 1 mimics non-unitarity in the first row of the CKM matrix if $|V_{ud}|$ is measured in β-decays of nuclei and $|V_{us}|$ is measured in $K \to \pi e\nu$ decays, since G_μ is regarded as the true Fermi constant in these measurements while it is G_β that is involved in the processes, and $|V_{ub}|^2$ is known to be smaller than experimental error of $|V_{us}|^2$. We therefore have

$$\frac{1}{\alpha_{22}^2 + |\alpha_{21}|^2} = \left(\frac{G_\beta}{G_\mu}\right)^2 \simeq |V_{ud}|^2 + |V_{us}|^2$$
$$\text{(measured in } K \to \pi e\nu \text{ decays)} + |V_{ub}|^2. \qquad (19)$$

Measurements of superallowed β-decays of nuclei yield the following experimental value [39]:

$$|V_{ud}| = 0.97417 \pm 0.00021. \qquad (20)$$

Combining measurements of the branching ratios of only three processes $K^\pm \to \pi^0 e\nu$, $K_L \to \pi^\pm e\nu$ and $K_S \to \pi^\pm e\nu$ [39], we obtain the following experimental value for $|V_{us}|$ times the kaon form factor, $f_+(0)$:

$$|V_{us}| f_+(0) = 0.21633 \pm 0.00055. \qquad (21)$$

The average of lattice calculations of the kaon form factor $f_+(0)$ in Refs. [40,41] is given by

$$f_+(0) = 0.9677 \pm 0.0037. \tag{22}$$

From Eqs. (20), (21) and (22), we obtain the following bound:

$$\frac{1}{\alpha_{22}^2 + |\alpha_{21}|^2} = 0.99898 \pm 0.00061. \tag{23}$$

- The mathematical inequality among α_{11}, α_{22} and α_{21} stems from the fact that the non-unitary mixing matrix N_{NU} is derived from the product of mixing matrices as in Eq. (12). The inequality reads [42–44]

$$4(1 - \alpha_{11})(1 - \alpha_{22}) > |\alpha_{21}|^2. \tag{24}$$

We combine the 3σ experimental bounds in Eqs. (18), (23) and the mathematical inequality Eq. (24), and we obtain the following 3σ bound[2]:

$$\alpha_{11} > 0.992573, \quad \alpha_{22} > 0.999589,$$
$$|\alpha_{21}| < 0.003494 \quad \text{at } 3\sigma. \tag{25}$$

To estimate the maximum significance of heavy neutrino mixing, we set the values of α_{11}, α_{22} and $|\alpha_{21}|$ at the above 3σ bounds and therefore employ a benchmark model with the following non-unitary mixing matrix N_{NU}:

$$N_{NU} = \begin{pmatrix} \alpha_{11} & 0 & 0 \\ \alpha_{21} & \alpha_{22} & 0 \\ 0 & 0 & 1 \end{pmatrix},$$
$$\alpha_{11} = 0.992573, \quad \alpha_{22} = 0.999589,$$
$$|\alpha_{21}| = 0.003494. \tag{26}$$

Since no experimental bound is reported on the phase of α_{21}, we leave it as a free parameter.

We comment in passing on constraints from past neutrino oscillation experiments. Among those experiments, the NOMAD experiment [45], a short baseline experiment searching for $\nu_\mu \rightarrow \nu_e$ and $\bar{\nu}_\mu \rightarrow \bar{\nu}_e$ transitions, gives the most severe bound, which is translated into the following:

$$2|\alpha_{21}|^2 \alpha_{11}^2 \leq 1.4 \times 10^{-3} \quad \text{at } 90\% \text{ confidence level.} \tag{27}$$

Our benchmark Eq. (26) satisfies the above bound.

---

[2] A different bound on α_{11}, α_{22} and $|\alpha_{21}|$ has been derived in Ref. [30] and used to determine a benchmark in Refs. [26–29], which takes into account experimental bounds on lepton flavor universality similar to Eqs. (18) and (23) and the NOMAD bound Eq. (27), but does not accommodate the mathematical inequality Eq. (24).

Finally, we mention constraints from lepton flavor violating processes. These constraints can always be evaded by tuning heavy neutrino mass $m_4, m_5, m_6, \ldots, m_N$ around the W boson mass, because the amplitude of a lepton flavor violating process involving charged leptons ℓ_α and ℓ_β, $A_{\alpha\beta}$, depends on N_{NU} through the following combination:

$$
\begin{aligned}
A_{\alpha\beta} &\propto \sum_{i=1}^{3} (N_{NU} U_{PMNS})_{\beta i} \, F\left(\frac{m_i}{M_W}\right) \left(U_{PMNS}^\dagger N_{NU}^\dagger\right)_{i\alpha} \\
&+ \sum_{j=4}^{N} (S_{3 \times N-3})_{\beta j} \, F\left(\frac{m_j}{M_W}\right) \left(S_{3 \times N-3}^\dagger\right)_{j\alpha} \\
&\simeq \left(N_{NU} N_{NU}^\dagger\right)_{\beta\alpha} F(0) \\
&+ \sum_{j=4}^{N} (S_{3 \times N-3})_{\beta j} \, F\left(\frac{m_j}{M_W}\right) \left(S_{3 \times N-3}^\dagger\right)_{j\alpha},
\end{aligned} \tag{28}
$$

where m_i, m_j are neutrino mass eigenvalues, M_W is the W boson mass, and $F(x)$ is a function depending on the process, and in the second line, we make the approximation with $m_1, m_2, m_3 \ll M_W$ as m_1, m_2, m_3 correspond to the tiny neutrino mass. It is evident that one can negate the term $(N_{NU} N_{NU}^\dagger)_{\beta\alpha} F(0)$ by taking appropriate $O(1)$ values for m_j / M_W ($j = 4, 5, 6, \ldots,$). We therefore neglect any constraints from lepton flavor violating processes.

In Appendix C, we consider another benchmark that satisfies the experimental bounds of Eqs. (18) and (23) at 2σ level as well as the mathematical inequality Eq. (24).

3.2 Simulation

We simulate the neutrino propagation and detection based on the benchmark model Eq. (26). The oscillation probability is calculated numerically with the formula Eq. (14) without making any approximation. For the standard oscillation parameters, we employ the central values of θ_{12}, θ_{13}, θ_{23}, Δm_{21}^2, $|\Delta m_{32}^2|$ found in the Particle Data Group [39]. As the CP-violating phase δ_{CP} and the sign of Δm_{32}^2 have not been measured conclusively, and the phase of α_{21}, $\text{Arg}(\alpha_{21})$, is undetermined in the benchmark, we repeat the simulation for various values of δ_{CP} and $\text{Arg}(\alpha_{21})$ and for both cases with $\Delta m_{32}^2 > 0$ and $\Delta m_{32}^2 < 0$. The values of the parameters used in the simulation are shown in Table 1.

We assume the baseline length L, fiducial volume, matter density along the baseline and neutrino beam off-axis angle [22,23,32] for the water Cerenkov detectors used in the T2HK, the T2HKK, the extension of the T2HK with a detector at Oki (T2HK+Oki), and the extension with the same detector at Kamioka (T2HK+Kami) as Table 2. The matter density is approximated to be uniform [32,46].

Table 1 Parameters used in our simulation

Physical parameter	Value in our simulation
$\sin^2\theta_{12}$	0.304
$\sin^2\theta_{13}$	0.0219
$\sin^2\theta_{23}$ (normal hierarchy)	0.51
$\sin^2\theta_{23}$ (inverted hierarchy)	0.50
Δm_{21}^2	7.53×10^{-5} eV^2
$|\Delta m_{32}^2|$ (normal hierarchy)	2.44×10^{-3}
$|\Delta m_{32}^2|$ (inverted hierarchy)	2.51×10^{-3}
δ_{CP}	Free
α_{11}	0.992573
$|\alpha_{21}|$	0.003494
α_{22}	0.999589
α_{31}	0
α_{32}	0
α_{33}	1
$\varphi_{21} = \arg(\alpha_{21})$	Free

We assume that J-PARC operates with 1.3 MW beam power for 10 years in the neutrino mode and for another 10 years in the antineutrino mode, delivering 27×10^{21} proton-on-target (POT) flux of neutrino-focusing beam and 27×10^{21} POT flux of antineutrino-focusing beam, as Table 3. The energy distributions of ν_μ and $\bar{\nu}_\mu$ in neutrino-focusing and antineutrino-focusing beams at each site are calculated based on Ref. [47]. ν_e and $\bar{\nu}_e$ components in the beam are ignored in this analysis. In Appendix A, we present the energy distributions.

The cross sections for charged current quasi-elastic scattering between a neutrino and a proton, $\nu_\ell n \rightarrow \ell^- p$, and that between an antineutrino and a neutron, $\bar{\nu}_\ell p \rightarrow \ell^+ n$, ($p$ and n denote proton and neutron, respectively, and ℓ denotes e or μ) are quoted from Ref. [48]. In Appendix B, we present the cross sections.

We assume the ideal measurement of ν_e and $\bar{\nu}_e$ and do not take into account acceptance and efficiency factors and finite energy resolution. Signals coming from processes other

Table 3 Flux of neutrino-focusing beam and antineutrino-focusing beam from J-PARC assumed

	Neutrino-focusing	Antineutrino-focusing
Flux	27×10^{21} POT	27×10^{21} POT

than charged current quasi-elastic scattering, as well as backgrounds due to neutral current quasi-elastic scatterings and other processes are not considered in the analysis.

The total numbers of neutrino events at the detectors at Kamioka, Oki and in Korea in the T2HK, T2HKK, T2HK+Oki, and T2HK+Kami with the detector size of Table 2 and the beam flux of Table 3 are tabulated in Table 4.

We calculate the numbers of ν_e and $\bar{\nu}_e$ events in 0.05 GeV bins of the neutrino energy E in the range 0.4 GeV $\leq E \leq$ 3 GeV for various values of δ_{CP} and $\text{Arg}(\alpha_{21})$ and for both cases with $\Delta m_{31}^2 > 0$ and $\Delta m_{31}^2 < 0$. We recall that in real experiments, the neutrino flux is determined by the measurement of ν_μ and $\bar{\nu}_\mu$ at the near detector, for which the standard oscillation is negligible but the non-unitary mixing reduces the ν_μ and $\bar{\nu}_\mu$ flux by the following amount:

$$P(\nu_\mu \rightarrow \nu_\mu)_{\text{near detector}} = P(\bar{\nu}_\mu \rightarrow \bar{\nu}_\mu)_{\text{near detector}}$$
$$= (N_{NU}N_{NU}^\dagger)_{\mu\mu} = |\alpha_{21}|^2 + \alpha_{22}^2. \quad (29)$$

In the analysis, we consider a virtual neutrino flux that is larger than the one found in Ref. [47] by $1/(|\alpha_{21}|^2 + \alpha_{22}^2)$, to compensate the reduction of Eq. (29). We therefore compute the number of events with a neutrino-focusing beam, $N_{e,i}$, and that with an antineutrino-focusing beam, $\tilde{N}_{e,i}$, as

for $i = 1, 2, 3, \ldots, 52$,
$$N_{e,i} = (\text{ Number of } \nu_e \text{ and } \bar{\nu}_e \text{ with } (0.4 + i \cdot 0.05) \text{ GeV}$$
$$\geq E \geq (0.4 + (i-1) \cdot 0.05) \text{ GeV })$$
$$= \int_{0.4+(i-1)\cdot 0.05 \, \text{GeV}}^{0.4+i\cdot 0.05 \, \text{GeV}} dE$$

Table 2 Parameters assumed for the detectors used in the experiments

Experiment	Site	Baseline length L (km)	Fiducial volume (kton)	Matter density ρ (g/cm^3)	Off-axis angle
T2HK	Kamioka	295	374	2.60	2.5°
T2HKK	Kamioka	295	187	2.60	2.5°
	Korea	1000	187	2.90	1.0°
T2HK+Oki	Kamioka	295	374	2.60	2.5°
	Oki	653	10	2.75	1.0°
T2HK+Kami	Kamoika	295	384	2.60	2.5°

Table 4 The total number of neutrino events at each detector, with the detector size of Table 2 and the beam flux of Table 3. The numbers for the neutrino-focusing beam and for the antineutrino-focusing beam are shown separately

Experiment	Detector	Number for neutrino-focusing beam	Number for antineutrino-focusing beam
T2HK	Kamioka	21×10^4	7.5×10^4
T2HKK	Kamioka	11×10^4	3.7×10^4
	Korea	3.1×10^4	1.7×10^4
T2HK+Oki 10 kton	Kamioka	21×10^4	7.5×10^4
	Oki	0.39×10^4	0.21×10^4
T2HK+Kami 10 kton	Kamioka	22×10^4	7.7×10^4
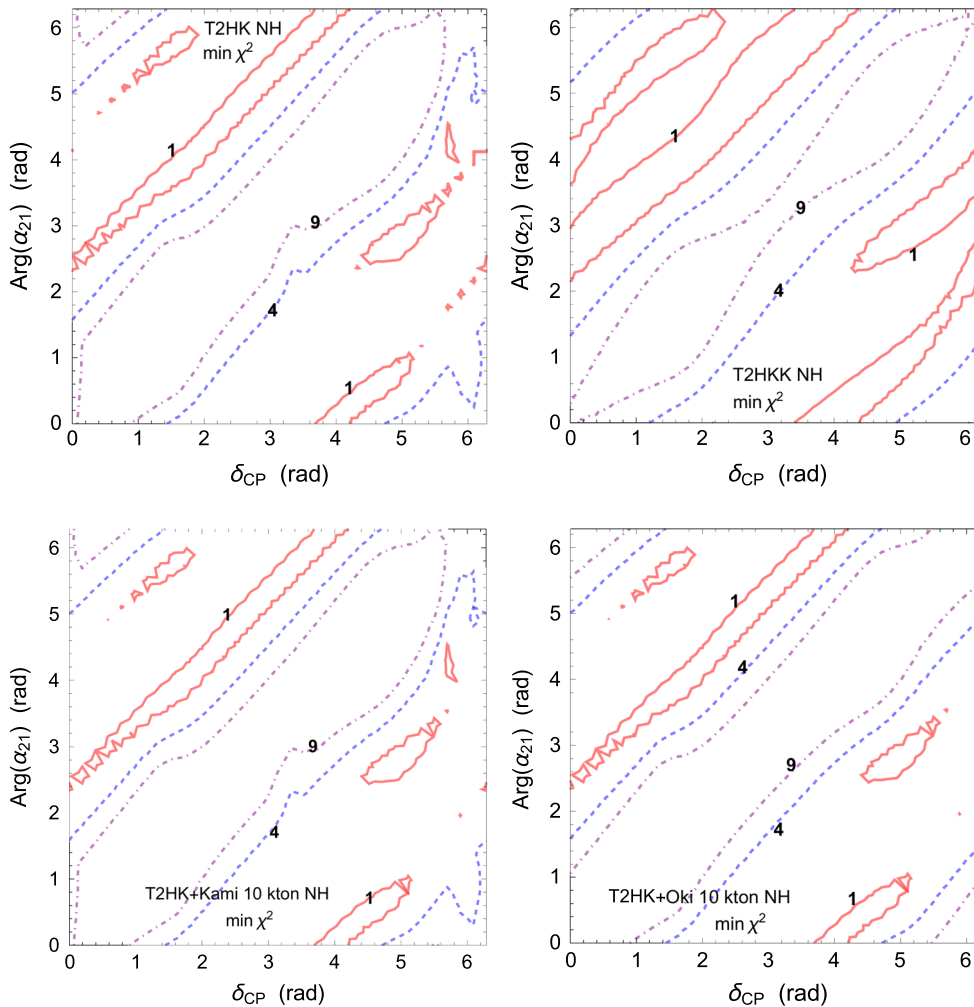
Fig. 1 The minimum of $\chi^2(\Pi)$ Eq. (32), min χ^2, on the plane of the standard CP-violating phase δ_{CP} and the new phase in the non-unitary mixing matrix Arg(α_{21}). The benchmark with Eq. (26) is assumed, and the true mass hierarchy is normal. The upper-left, upper-right and lower-right subplots correspond to the T2HK, the T2HKK, and the plan of the T2HK plus a 10 kton water Cerenkov detector at Oki, respectively. For comparative study, we show in the lower-left a subplot for a plan of the T2HK plus a 10 kton water Cerenkov detector at Kamioka. min $\chi^2 = 1, 4, 9$ on the red solid, blue dashed, and purple dot-dashed contours, respectively

$$\times \left\{ \frac{\Phi_{\nu_\mu}(E)}{|\alpha_{21}|^2 + \alpha_{22}^2} P(\nu_\mu \to \nu_e; E) N_n \, \sigma(\nu_e n \to e^- p; E) \right.$$
$$\left. + \frac{\Phi_{\bar{\nu}_\mu}(E)}{|\alpha_{21}|^2 + \alpha_{22}^2} P(\bar{\nu}_\mu \to \bar{\nu}_e; E) N_p \, \sigma(\bar{\nu}_e p \to e^+ n; E) \right\},$$

$$\tilde{N}_{e,i} = (\Phi_{\nu_\mu} \to \tilde{\Phi}_{\nu_\mu} \text{ and } \Phi_{\bar{\nu}_\mu} \to \tilde{\Phi}_{\bar{\nu}_\mu} \text{ in above}), \quad (30)$$

where $\Phi_{\nu_\mu}(E)$ and $\Phi_{\bar{\nu}_\mu}(E)$, respectively, denote the neutrino and antineutrino flux per energy in a neutrino-focusing beam, and $\tilde{\Phi}_{\nu_\mu}(E)$ and $\tilde{\Phi}_{\bar{\nu}_\mu}(E)$ are those in an antineutrino-
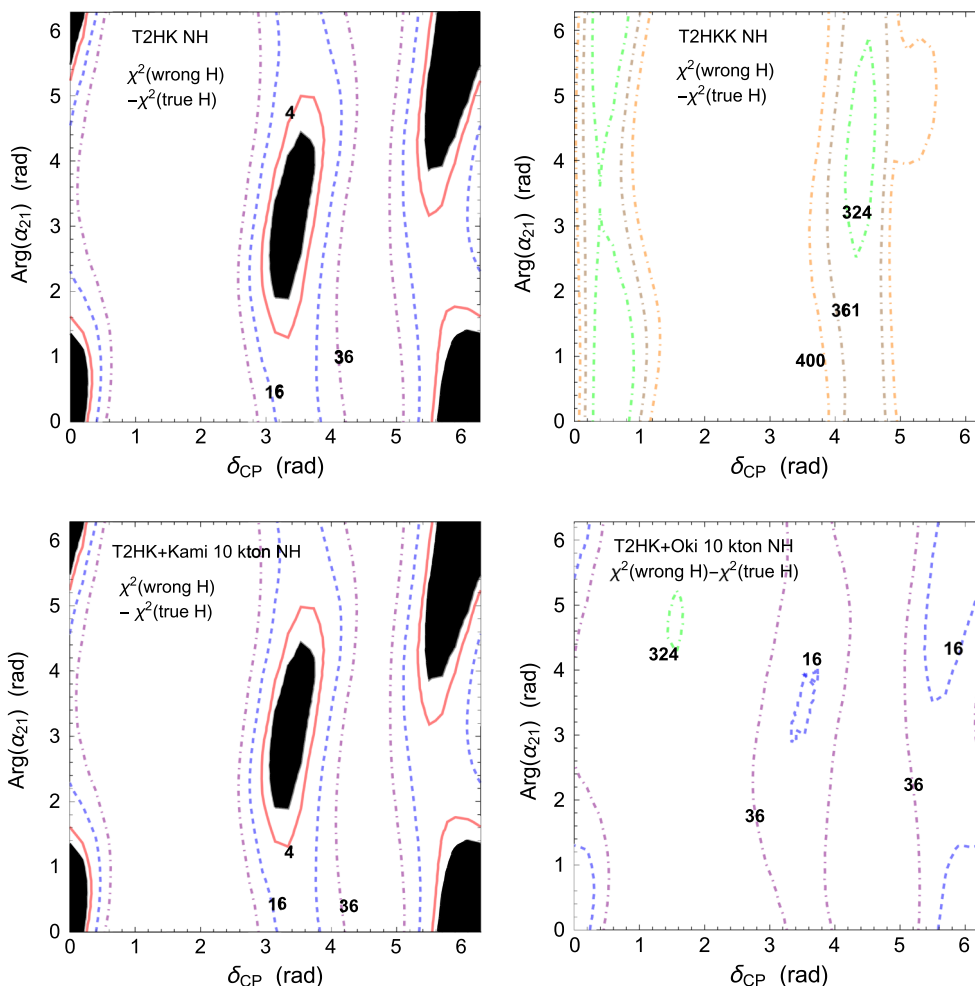
Fig. 2 The difference between the minima (with respect to δ_{CP} only) of $\chi^2(\Pi)$ for the wrong and true mass hierarchies, {min χ^2(wrong H) − min χ^2(true H)}. The benchmark with Eq. (26) is assumed, and the true mass hierarchy is normal. The upper-left, upper-right and lower-right subplots correspond to the T2HK, the T2HKK, and the plan of the T2HK plus a 10 kton water Cerenkov detector at Oki, respectively. For comparative study, we show in the lower-left a subplot for a plan of the T2HK plus a 10 kton water Cerenkov detector at Kamioka. {min χ^2(wrong H) − min χ^2(true H)} = 4, 16, 36 on the red solid, blue dashed, and purple dot-dashed contours, respectively, and {min χ^2(wrong H) − min χ^2(true H)} = 18^2, 19^2, 20^2 on the green, brown, and orange dot-dashed contours, respectively. The black-filled regions are where the wrong mass hierarchy is favored over the true mass hierarchy, i.e., min χ^2(wrong H) − min χ^2(true H) < 0

focusing beam. P denotes the transition probability Eq. (14), with E dependence made explicit. N_n and N_p are, respectively, the number of neutrons and protons in a water Cerenkov detector. σ denotes the cross sections for $\nu_\ell n \rightarrow \ell^- p$ and $\bar{\nu}_\ell p \rightarrow \ell^+ n$ processes.

3.3 χ^2 analysis

We fit the numbers of events in the bins with neutrino-focusing and antineutrino-focusing beams, detected at Kamioka/Korea/Oki, $N_{e,i,\text{site}}$ and $\tilde{N}_{e,i,\text{site}}$ ($i = 1, 2, \ldots, 52$) (site=Kamioka, Korea, Oki), under the assumption that no heavy neutrino mixing is present, that is, $N_{NU} = I_3$. This is performed by minimizing $\chi^2(\Pi)$,

$$\chi^2(\Pi) = \chi^2_{\text{statistical}}(\Pi) + \chi^2_{\text{parametrical}}(\Pi) + \chi^2_{\text{systematic}},$$

$$\chi^2_{\text{statistical}}(\Pi) = \sum_{\text{site}} \sum_{i=1}^{52} \left\{ \frac{\left(N_{e,i,\text{site}} - N_{e,i,\text{site}}^{\text{unitary}}(\Pi)\right)^2}{N_{e,i,\text{site}}} + \frac{\left(\tilde{N}_{e,i,\text{site}} - \tilde{N}_{e,i,\text{site}}^{\text{unitary}}(\Pi)\right)^2}{\tilde{N}_{e,i,\text{site}}} \right\}, \quad (31)$$

with respect to the standard oscillation parameters $\Pi = (\theta_{12}, \theta_{13}, \theta_{23}, \Delta m_{21}^2, \Delta m_{32}^2, \delta_{CP})$. Here, $\chi^2_{\text{statistical}}$ represents statistical uncertainty, $N_{e,i,\text{site}}^{\text{unitary}}(\Pi)$ is the number of ν_e and
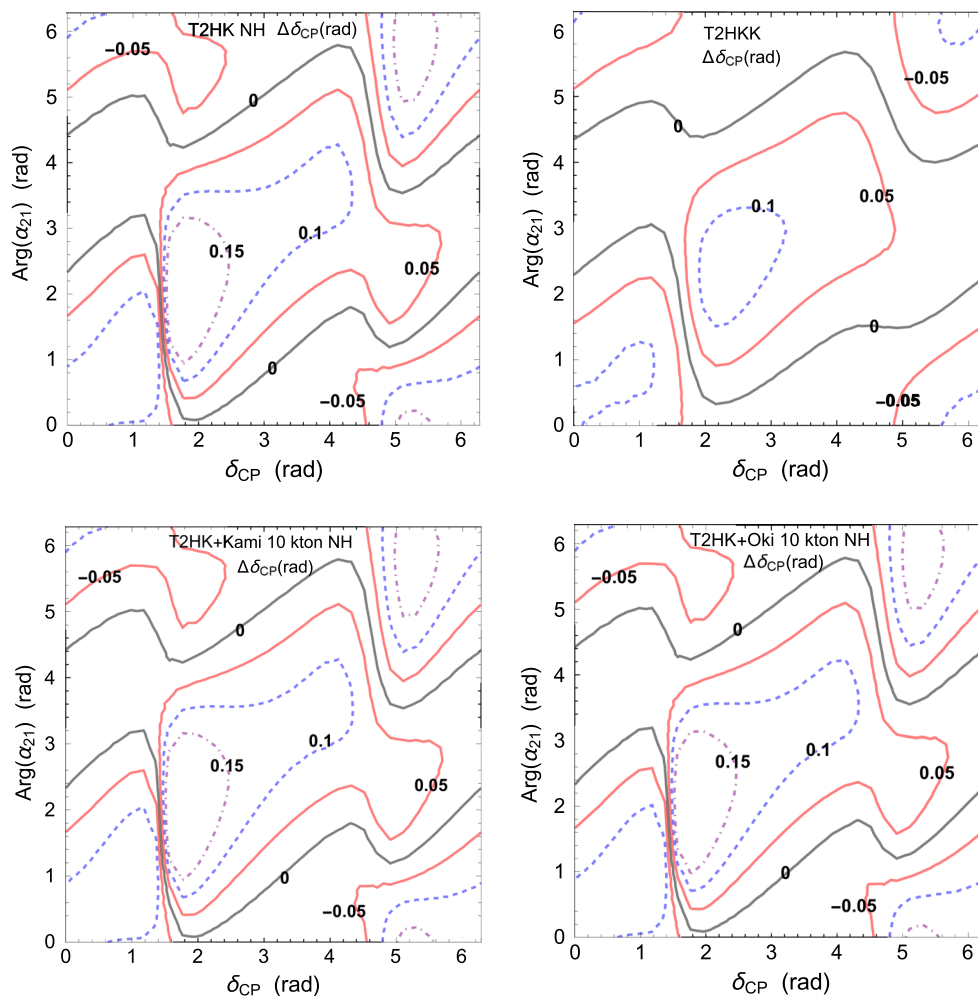
Fig. 3 The difference between the true value of δ_{CP}, and the value that minimizes $\chi^2(\Pi)$ of Eq. (32) with true mass hierarchy. The benchmark with Eq. (26) is assumed, and the true mass hierarchy is normal. The upper-left, upper-right and lower-right subplots correspond to the T2HK, the T2HKK, and the plan of the T2HK plus a 10 kton water Cerenkov detector at Oki, respectively. For comparative study, we show in the lower-left a subplot for a plan of the T2HK plus a 10 kton water Cerenkov detector at Kamioka. $|\Delta\delta_{CP}| = 0$, 0.05rad, 0.1rad, and 0.15rad on the black solid, red solid, blue dashed, and purple dot-dashed contours, respectively

$\bar{\nu}_e$ events in a bin with a neutrino-focusing beam when $N_{NU} = I_3$, calculated as a function of the standard oscillation parameters Π, and $\tilde{N}_{e,i,\text{site}}^{\text{unitary}}(\Pi)$ is the corresponding number with an antineutrino-focusing beam.

The following simplification is made for $\chi^2_{\text{parametrical}}(\Pi)$: we note that θ_{12}, θ_{13}, θ_{23}, Δm_{21}^2, $|\Delta m_{32}^2|$ can be accurately measured in disappearance experiments with $\bar{\nu}_e \rightarrow \bar{\nu}_e$, $\nu_\mu \rightarrow \nu_\mu$ and $\bar{\nu}_\mu \rightarrow \bar{\nu}_\mu$, which are not influenced by heavy neutrino mixing as parametrized by N_{NU}, because N_{NU} equally affects the neutrino flux of the same flavor at the near and far detectors. ($\cos \delta_{CP}$ and the sign of Δm_{32}^2 are also possibly measured in disappearance experiments, but the sensitivity is limited.) We therefore assume that the true values of θ_{12}, θ_{13}, θ_{23}, Δm_{21}^2, $|\Delta m_{32}^2|$ are known prior to the experiments considered in this paper, and accordingly we fix

θ_{12}, θ_{13}, θ_{23}, Δm_{21}^2, $|\Delta m_{32}^2|$ in $\chi^2(\Pi)$ at the values used in the simulation and set $\chi^2_{\text{parametrical}}(\Pi) = 0$.

Finally, we have $\chi^2_{\text{systematic}} = 0$ in the current analysis, because no acceptance, efficiency, energy resolution and background events are considered.

To summarize, $\chi^2(\Pi)$ is approximated by

$$\chi^2(\Pi) = \chi^2_{\text{statistical}}\left(\delta_{CP}, \text{sgn}\left(\Delta m_{32}^2\right)\right)$$

with θ_{12}, θ_{13}, θ_{23}, Δm_{21}^2, $|\Delta m_{32}^2|$ given in Table 1. (32)

We numerically evaluate the minimum of $\chi^2(\Pi)$ Eq. (32), which corresponds to the square of the significance for heavy neutrino mixing. In Fig. 1, we show contour plots of the minimum of $\chi^2(\Pi)$,
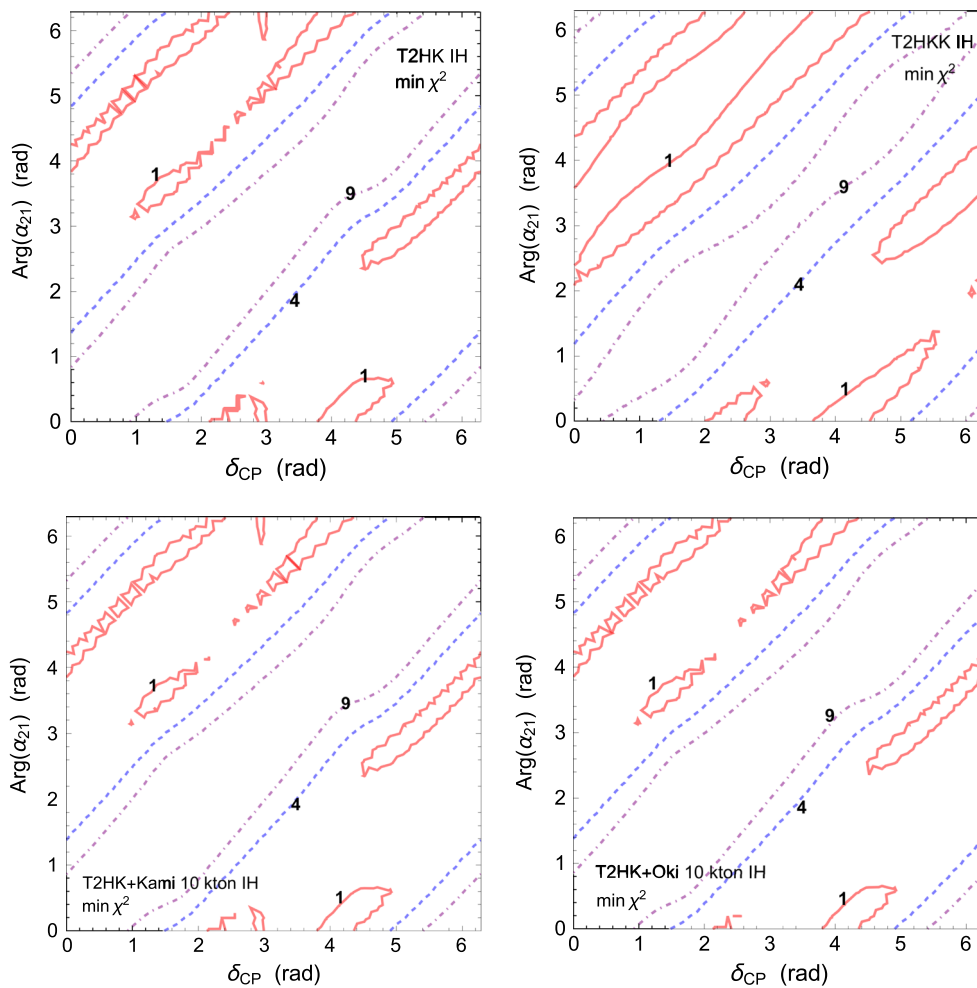
Fig. 4 The minimum of $\chi^2(\Pi)$ Eq. (32), min χ^2. The benchmark with Eq. (26) is assumed, and the true mass hierarchy is inverted. The upper-left, upper-right and lower-right subplots correspond to the T2HK, the T2HKK, and the plan of the T2HK plus a 10 kton water Cerenkov detec-tor at Oki, respectively. For comparative study, we show in the lower-left a subplot for a plan of the T2HK plus a 10 kton water Cerenkov detector at Kamioka. min $\chi^2 = 1$, 4, 9 on the red solid, blue dashed, and purple dot-dashed contours, respectively

$$\text{min } \chi^2 \equiv \min \left\{ \min_{\delta_{CP}} \chi^2(\delta_{CP}, \ \Delta m_{32}^2 > 0), \right.$$
$$\left. \min_{\delta_{CP}} \chi^2\left(\delta_{CP}, \ \Delta m_{32}^2 < 0\right) \right\}, \tag{33}$$

on the plane spanned by the CP-violating phase in the PMNS matrix δ_{CP} and the phase in the non-unitary mixing matrix Arg(α_{21}), when the true mass hierarchy is normal. The four subplots correspond to the T2HK, the T2HKK, the extension of the T2HK with a detector at OKi, and that with the same detector at Kamioka.

We study the impact of heavy neutrino mixing on the mass hierarchy measurement that is performed by fitting data without incorporating heavy neutrino mixing. For this purpose, we evaluate the difference between the minimum (with respect to δ_{CP} only) of $\chi^2(\Pi)$ for the wrong hierarchy and that for the true mass hierarchy, which corresponds to the square of the significance of rejecting the wrong mass hierarchy. We show in Fig. 2 contour plots of the difference,

$$\text{min } \chi^2(\text{wrong H}) - \text{min } \chi^2(\text{true H})$$
$$\equiv \min_{\delta_{CP}} \chi^2\left(\delta_{CP}, \ \text{wrong sgn}\left(\Delta m_{32}^2\right)\right)$$
$$- \min_{\delta_{CP}} \chi^2\left(\delta_{CP}, \ \text{true sgn}\left(\Delta m_{32}^2\right)\right), \tag{34}$$

on the same plane when the true mass hierarchy is normal. The black-filled regions in the left subplots are where the wrong mass hierarchy is favored over the true mass hierarchy, i.e., min $\chi^2(\text{wrong H}) - \text{min } \chi^2(\text{true H}) < 0$.

We study the impact of heavy neutrino mixing on the value of δ_{CP} that minimizes $\chi^2(\Pi)$. To assess the impact, we compute the difference between the true value of δ_{CP}, and the value that minimizes $\chi^2(\Pi)$ of Eq. (32) with the true mass
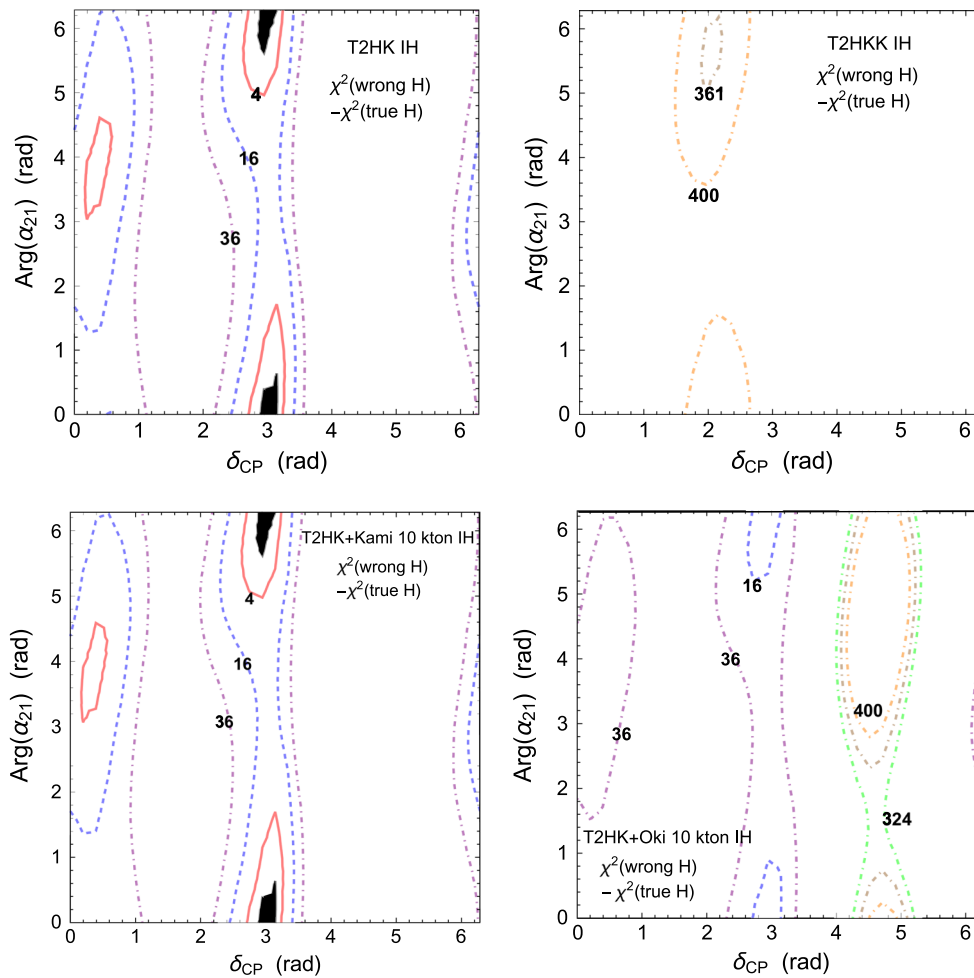
Fig. 5 The difference between the minima (with respect to δ_{CP} only) of $\chi^2(\Pi)$ for the wrong and true mass hierarchy, {min χ^2(wrong H) − min χ^2(true H)}, which is the square of the significance of rejecting the wrong hierarchy. The benchmark with Eq. (26) is assumed, and the true mass hierarchy is inverted. The upper-left, upper-right and lower-right subplots correspond to the T2HK, the T2HKK, and the plan of the T2HK plus a 10 kton water Cerenkov detector at Oki, respectively. For comparative study, we show in the lower-left a sub-plot for a plan of the T2HK plus a 10 kton water Cerenkov detector at Kamioka. {min χ^2(wrong H) − min χ^2(true H)} = 4, 16, 36 on the red solid, blue dashed, and purple dot-dashed contours, respectively, and {min χ^2(wrong H) − min χ^2(true H)} = 18^2, 19^2, 20^2 on the green, brown, and orange dot-dashed contours, respectively. The black-filled regions are where the wrong mass hierarchy is favored over the true mass hierarchy, i.e., min χ^2(wrong H) − min χ^2(true H) < 0

hierarchy. We show in Fig. 3 contour plots of the difference,

$$\Delta\delta_{CP} \equiv \left(\delta_{CP} \text{ that minimizes } \chi^2\left(\delta_{CP}, \text{ true sgn}\left(\Delta m^2_{32}\right)\right)\right)$$
$$- (\text{true } \delta_{CP}) \tag{35}$$

on the same plane when the true mass hierarchy is normal.

Figures 4, 5, 6 are the corresponding figures when the true mass hierarchy is inverted.

The following observations are made:

(A) In Figs. 1 and 4, we see that the significance of heavy neutrino mixing can be above 3σ for Arg(α_{21}) ∼ δ_{CP}, but decreases considerably for Arg(α_{21}) ≃ $\delta_{CP} \pm \pi/2$

in all the experiments, confirming that the sensitivity deteriorates due to suppression of interference between the standard oscillation amplitude and non-unitary mixing α_{21} at the first oscillation peak, as can be read from Eqs. (5) and (6). The regions of depleted sensitivity is slightly off the lines Arg(α_{21}) = $\delta_{CP} \pm \pi/2$, because of the influence of the second, subleading interference term in Eqs. (5) and (6). We also find that the significance does not ameliorate in the T2HKK and in the extension of the T2HK with a 10 kton detector at Oki. Rather, the T2HKK shows inferior performance due to the loss of statistics, which is seen in Table 4.
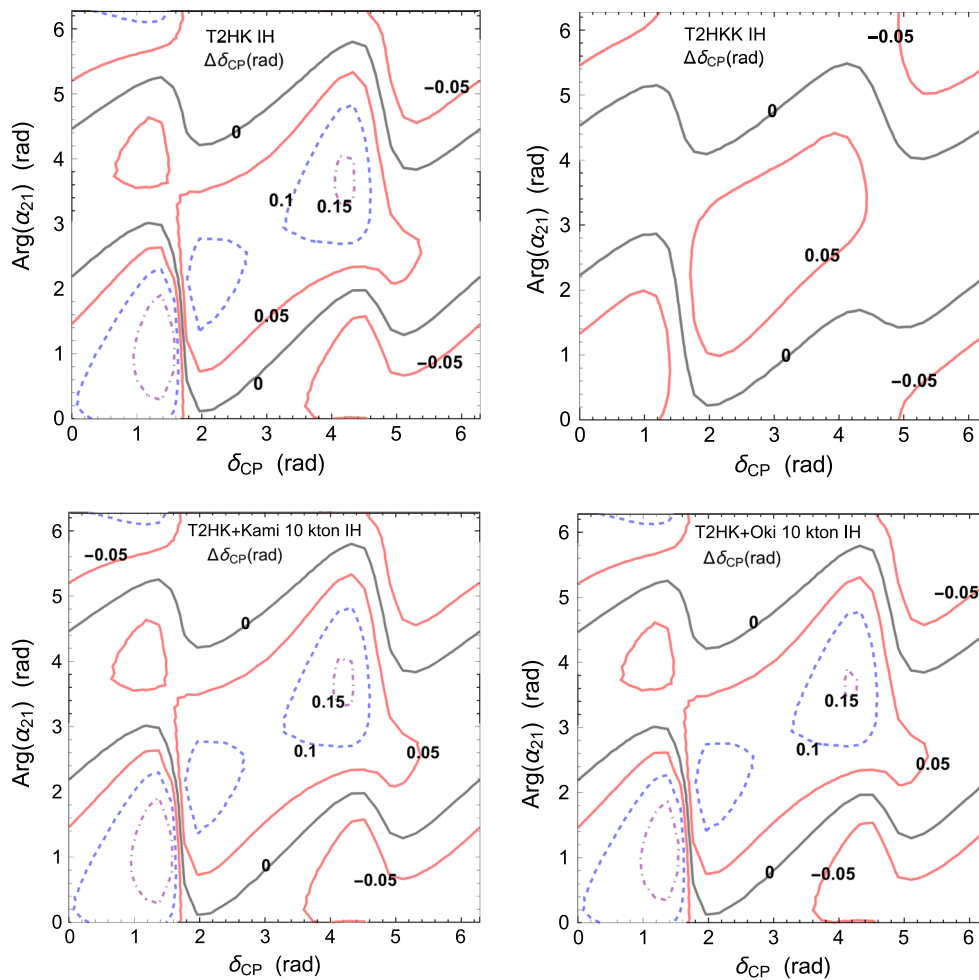
Fig. 6 The difference between the true value of δ_{CP}, and the value that minimizes $\chi^2(\Pi)$ of Eq. (32) with the true mass hierarchy. The benchmark with Eq. (26) is assumed, and the true mass hierarchy is inverted. The upper-left, upper-right and lower-right subplots correspond to the T2HK, the T2HKK, and the plan of the T2HK plus a 10 kton water Cerenkov detector at Oki, respectively. For comparative study, we show in the lower-left a subplot for a plan of the T2HK plus a 10 kton water Cerenkov detector at Kamioka. $|\Delta\delta_{CP}| = 0$, 0.05 rad, 0.1 rad, and 0.15 rad on the black solid, red sold, blue dashed, and purple dot-dashed contours, respectively

(B) In Figs. 2 and 5, we observe that in the T2HK, the wrong mass hierarchy is favored when $(\delta_{CP}, \text{Arg}(\alpha_{21})) \sim (0, 0)$, (π, π) holds in the normal hierarchy case, and when $(\delta_{CP}, \text{Arg}(\alpha_{21})) \sim (\pi, 0)$ holds in the inverted hierarchy case. To estimate the impact of non-unitary mixing on the mass hierarchy measurement in the T2HK, we show in Fig. 7 the values of $\{\min \chi^2(\text{wrong H}) - \min \chi^2(\text{true H})\}$ when non-unitarity is absent, i.e. $N_{NU} = I$, calculated with the same procedure as Figs. 2 and 5.

Comparison of Figs. 2 and 5 with Fig. 7 indicates that, for $\delta_{CP} \sim 0, \pi$, the T2HK has limited sensitivity to the mass hierarchy in the unitary case, and the presence of non-unitary mixing may aggravate it to the extent that the wrong mass hierarchy is favored. Such impact of non-unitary

mixing is because α_{21} cancels matter effects in the neutrino transition probability Eq. (3) when $(\delta_{CP}, \text{Arg}(\alpha_{21})) \sim (0, 0)$, (π, π) holds in the normal hierarchy case, and when $(\delta_{CP}, \text{Arg}(\alpha_{21})) \sim (\pi, 0)$ holds in the inverted hierarchy case. Although α_{21} and matter effects add positively in the antineutrino transition probability Eq. (4) in the same cases, it does not change the situation because neutrino flux is larger than antineutrino flux in our setup (see Table 3 and Fig. 9).

The T2HKK maintains strong sensitivity to the mass hierarchy in the presence of heavy neutrino mixing. Also, adding a 10 kton detector at Oki to the T2HK drastically ameliorates sensitivity to the mass hierarchy, in spite of the small size of the Oki detector. The advantage of the T2HKK and T2HK+Oki is because measurements with different matter effects resolve degeneracy between non-unitary mixing α_{21} and matter effects.
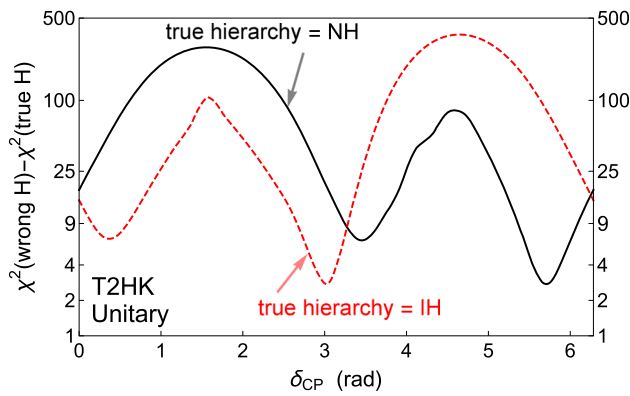
Fig. 7 The difference between the minima (with respect to δ_{CP} only) of $\chi^2(\Pi)$ for the wrong and true mass hierarchy, {min χ^2(wrong H) − min χ^2(true H)}, when the neutrino mixing is unitary (no heavy neutrino mixing is present), in the T2HK. The results are presented as functions of the true value of δ_{CP}. The black solid line corresponds to the case when the true hierarchy is normal, and the red dashed line to the case when the true hierarchy is inverted

We stress that even a small 10 kton detector at Oki negates the impact of heavy neutrino mixing on the mass hierarchy measurement and allows for correct measurement.

(C) In Figs. 3 and 6, we find that the value of δ_{CP} that minimizes χ^2 under the assumption of standard unitary oscillation can deviate from the true δ_{CP} by more than 0.15 radian in the T2HK, and by more than 0.1 radian in the T2HKK. The result should be compared to the resolution of δ_{CP}. To this end, we present in Fig. 8 the difference between δ_{CP} that gives $\chi^2 = 1$ and the true δ_{CP} when non-unitarity is absent ($N_{NU} = I$),

$$(\Delta\delta_{CP} \text{ at } 1\sigma) \equiv (\delta_{CP} \text{ that gives } \chi^2 = 1) - (\text{true } \delta_{CP}), \tag{36}$$

which quantifies 1σ resolution of the δ_{CP} measurement in the standard oscillation case. Equation (36) is calculated through a simulation performed with the same procedure.

1σ resolution for δ_{CP} is better than 0.1 radian in the T2HK and than 0.08 radian in the T2HKK[3], which is of the same order as the deviation of δ_{CP} due to non-unitarity. This indicates that non-unitarity can have a non-negligible effect on the δ_{CP} measurement, and hence, if a hint of non-unitarity has been discovered, it must be incorporated in the data fitting in order to measure δ_{CP} correctly.

The deviation due to non-unitarity is enhanced when (true δ_{CP}) $\sim$ Arg(α_{21}) holds. This is because interference

---

[3] The tendency that the T2HKK has a better sensitivity to δ_{CP} than the T2HK in the standard oscillation case is also observed in Ref. [23].

between the part of the standard oscillation amplitude proportional to $e^{i\delta_{CP}}$ and the amplitude involving non-unitary mixing α_{21} is maximized, and so is the influence of α_{21} on the value of δ_{CP} that minimizes χ^2.

The deviation is smaller in the T2HKK than in the T2HK. This is due to the fact that the energy dependence of the part of the standard oscillation amplitude proportional to $e^{i\delta_{CP}}$, which helps distinguish the standard and non-unitary amplitudes, is more accurately measured with a longer baseline. Hence, the δ_{CP} measurement is less affected by non-unitarity in the T2HKK.

4 Summary

We have studied the discovery potential for the mixing of heavy isospin-singlet neutrinos in the Tokai-to-Hyper-Kamiokande (T2HK), the Tokai-to-Hyper-Kamiokande-to-Korea (T2HKK), and a plan of adding a small detector at Oki Islands to the T2HK, and further examined the feasibility of measuring the mass hierarchy and the standard CP-violating phase δ_{CP} in the presence of heavy neutrino mixing by fitting data without assuming heavy neutrino mixing. The mixing of heavy neutrinos is parametrized with a non-unitary mixing matrix for active flavors. A benchmark that maximizes the non-unitary mixing and is consistent with the current experimental and theoretical bounds is employed to estimate the largest possible significance of heavy neutrino mixing and its impact on the mass hierarchy and δ_{CP} measurement.

Through a simulation, we have revealed that the significance of heavy neutrino mixing can be above 3σ in all the experiments when the standard phase δ_{CP} and a new CP-violating phase originating from heavy neutrino mixing, Arg(α_{21}), satisfy Arg(α_{21}) $\simeq \delta_{CP}$. The significance decreases considerably for Arg(α_{21}) $\simeq \delta_{CP} \pm \pi/2$, due to suppression of interference between the standard oscillation amplitude and a non-unitary mixing term.

In the T2HK, the mass hierarchy measurement is so affected by heavy neutrino mixing that the wrong mass hierarchy is favored for (δ_{CP}, Arg(α_{21})) $\sim$ (0, 0), (π, π) in the normal hierarchy case, and for (δ_{CP}, Arg(α_{21})) $\sim$ (π, 0) in the inverted hierarchy case. This is because a non-unitary mixing term possibly cancels matter effects. In contrast, the T2HKK and the extension of the T2HK with a 10 kton detector at Oki show strong sensitivity to the mass hierarchy even with heavy neutrino mixing, because measurements with different baseline lengths at Kamioka and in Korea or at Oki resolve degeneracy between a non-unitary mixing term and matter effects. We thus conclude that (i) the mass hierarchy measurement in the T2HKK is highly stable against any effects of heavy neutrino mixing, and that (ii) although the mass hierarchy measurement in the T2HK is easily affected,
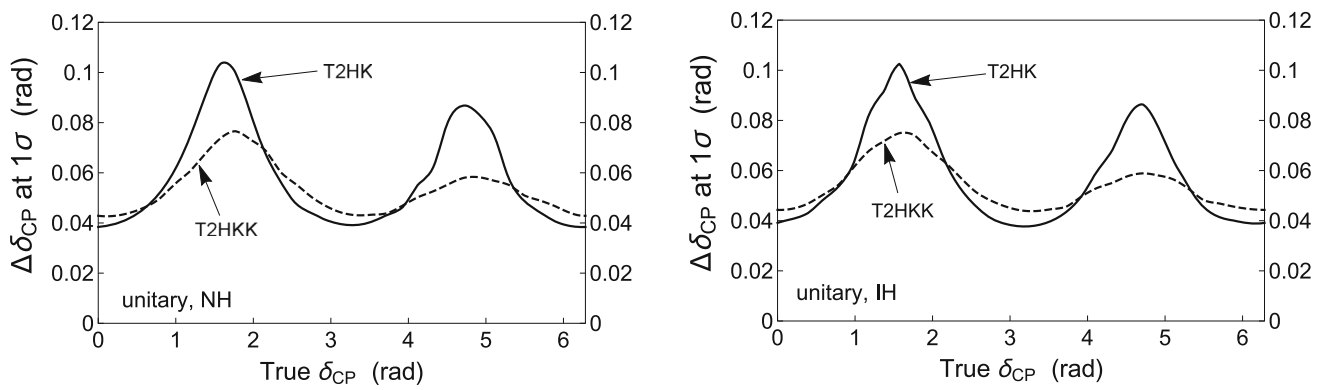
Fig. 8 The resolution of the δ_{CP} measurement when non-unitarity is absent, quantified as the difference between δ_{CP} that gives $\chi^2 = 1$ and the true δ_{CP} Eq. (36). The results are presented as functions of the true δ_{CP}. The left and right plots correspond to the cases when the true

mass hierarchy is normal and inverted, respectively. In each plot, the solid line indicates the sensitivity in the T2HK, and the dashed line the sensitivity in the T2HKK

the addition of a small detector at Oki negates effects of heavy neutrino mixing.

In the presence of non-unitarity, the value of δ_{CP} measured without incorporating non-unitarity deviates from the true δ_{CP}. The deviation is enhanced when $\text{Arg}(\alpha_{21})$ is close to the true δ_{CP}, because in such a case, the part of the standard oscillation amplitude proportional to $e^{i\delta_{CP}}$ interferes maximally with a non-unitary mixing term at oscillation peaks. The deviation can be of the same order as 1σ resolution of the δ_{CP} measurement, which suggests that if a hint of non-unitarity has been discovered, one must employ an appropriate ansatz including the non-unitary mixing terms to fit neutrino oscillation data and measure δ_{CP}.

Appendix A

In Fig. 9, we show the flux of ν_μ and $\bar{\nu}_\mu$ in neutrino-focusing and antineutrino-focusing beams from J-PARC, detected at a water Cerenkov detector at Kamioka, Oki and in Korea if the neutrino oscillation were absent. The baseline length and beam off-axis angle assumed are given in Table 2. In each plot, the blue lines correspond to a neutrino-focusing beam and the red lines correspond to an antineutrino-focusing beam. The solid lines denote ν_μ flux and the dashed lines denote $\bar{\nu}_\mu$ flux.
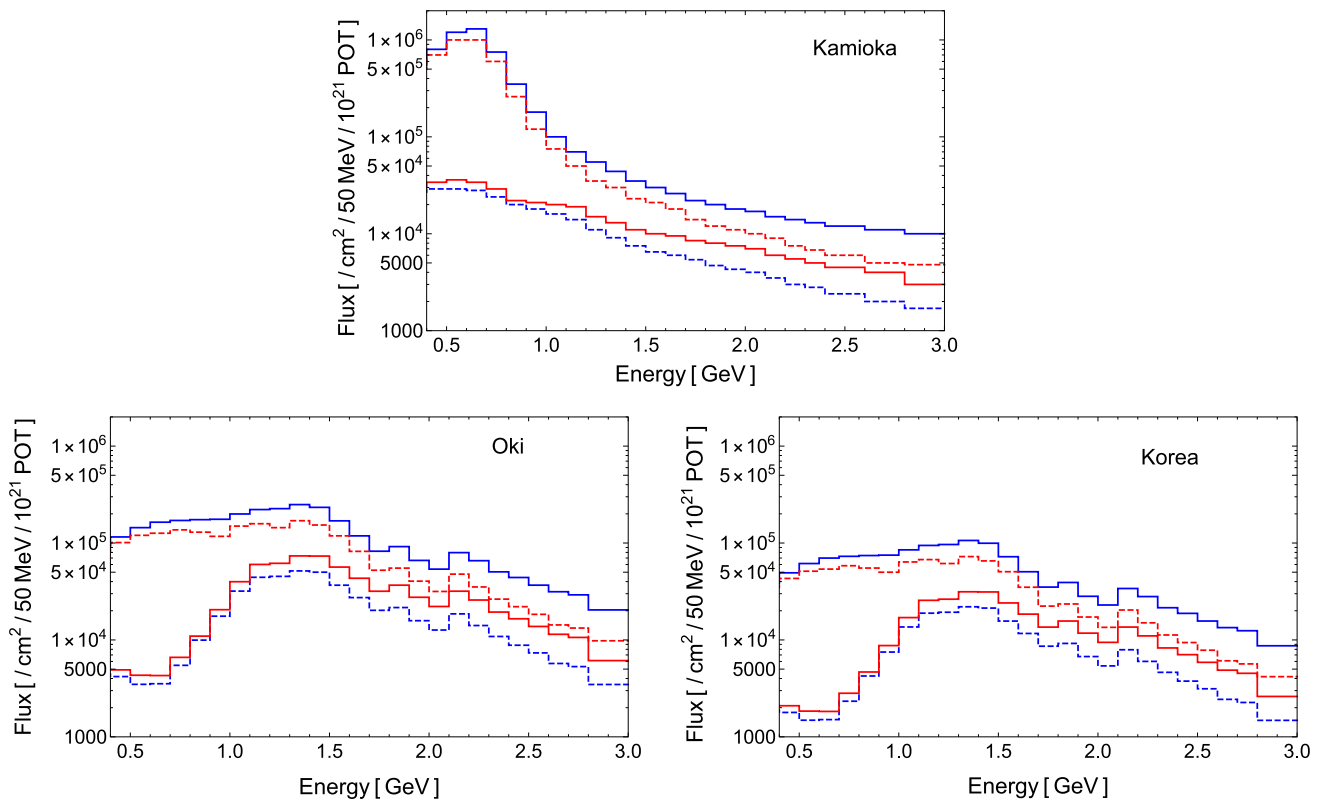
Fig. 9 Flux of ν_μ and $\bar{\nu}_\mu$ in neutrino-focusing and antineutrino-focusing beams detected at a water Cerenkov detector at Kamioka, Oki and in Korea if the neutrino oscillation were absent. The upper plot, the lower-left plot and the lower-right plot, respectively, correspond to Kamioka, Oki and Korea. In each plot, the blue lines correspond to a neutrino-focusing beam and the red lines correspond to an antineutrino-focusing beam. The solid lines denote ν_μ flux and the dashed lines denote $\bar{\nu}_\mu$ flux

Appendix B

In Fig. 10, we show the cross sections for charged current quasi-elastic scatterings $\nu_\ell n \to \ell^- p$ and $\bar{\nu}_\ell p \to \ell^+ n$ ($\ell = e$, μ). The solid line corresponds to the cross section for ν_ℓ, and the dashed line to that for $\bar{\nu}_\ell$.
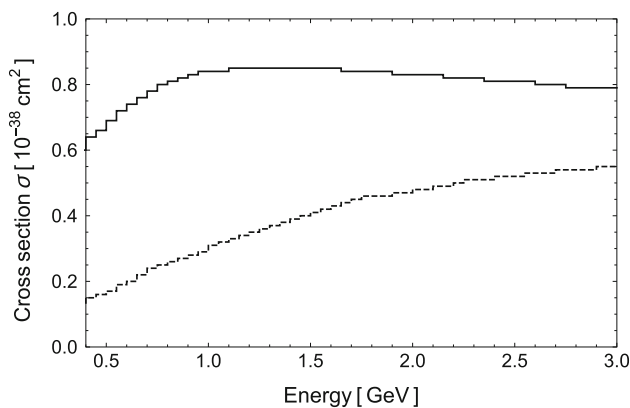
Fig. 10 The cross section for charged current quasi-elastic scatterings $\nu_\ell n \to \ell^- p$ and $\bar{\nu}_\ell p \to \ell^+ n$ ($\ell = e$, μ). The solid line corresponds to the cross section for ν_ℓ, and the dashed line to that for $\bar{\nu}_\ell$

Appendix C

We consider an alternative benchmark with a smaller non-unitary mixing that satisfies the experimental bounds Eqs. (18) and (23) at 2σ level as well as the mathematical inequality Eq. (24). The non-unitary mixing matrix in the new benchmark is given by

$$N_{NU} = \begin{pmatrix} \alpha_{11} & 0 & 0 \\ \alpha_{21} & \alpha_{22} & 0 \\ 0 & 0 & 1 \end{pmatrix},$$

$$\alpha_{11} = 0.994486, \quad \alpha_{22} = 0.999897, \quad |\alpha_{21}| = 0.002343. \tag{37}$$

Based on the benchmark with Eq. (37), we repeat the same simulation and calculation as Sects. 3.2 and 3.3, and obtain the results in Figs. 11, 12, 13, 14, 15 and 16.

The plots for $\min \chi^2$, Figs. 11 and 14, show that the significance of non-unitary mixing is reduced below 3σ in most parameter regions in the T2HK and in the entire region in the T2HKK. The dependence on (δ_{CP}, $\mathrm{Arg}(\alpha_{21})$) is similar to the plots for the original benchmark, Figs. 1 and 4.
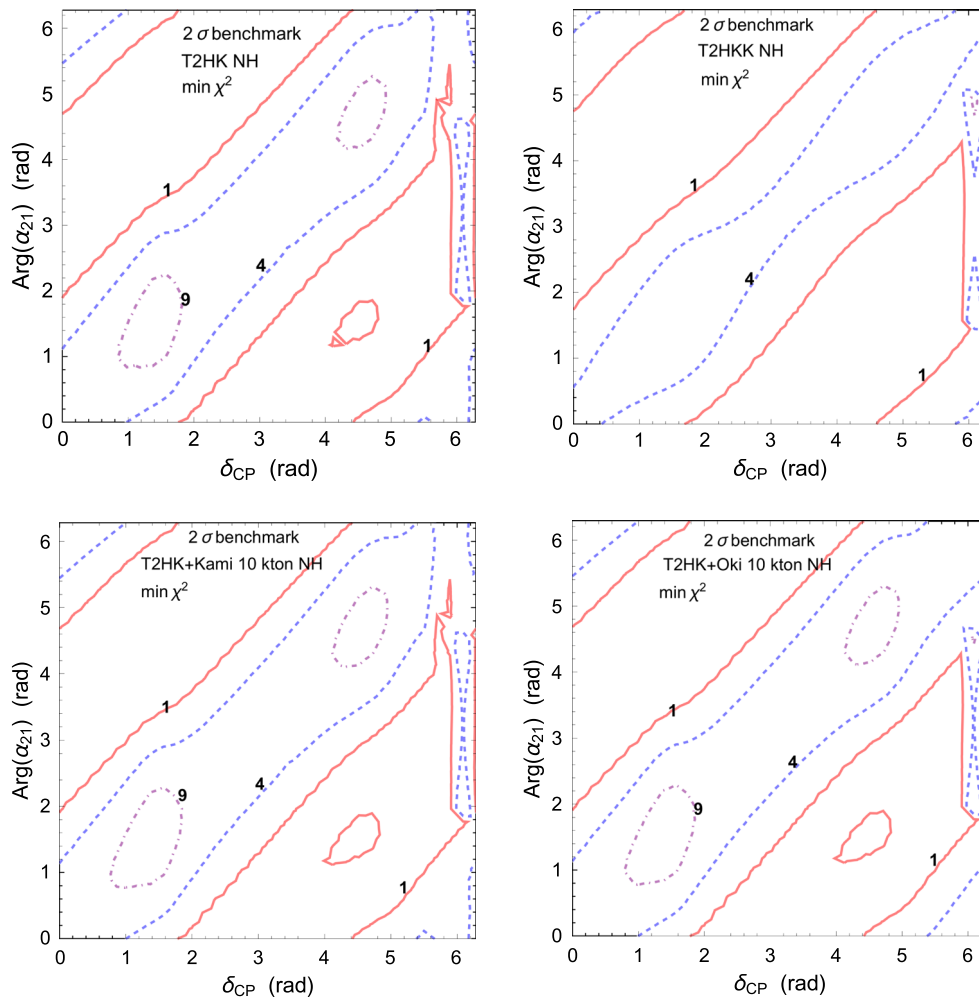
Fig. 11 The minimum of $\chi^2(\Pi)$ Eq. (32), min χ^2, on the plane of δ_{CP} and Arg(α_{21}). The benchmark with Eq. (37) is assumed, and the true mass hierarchy is normal. The upper-left, upper-right and lower-right subplots correspond to the T2HK, the T2HKK, and the plan of the T2HK plus a 10 kton water Cerenkov detector at Oki, respectively. For comparative study, we show in the lower-left a subplot for a plan of the T2HK plus a 10 kton water Cerenkov detector at Kamioka. min $\chi^2 = 1$, 4, 9 on the red solid, blue dashed, and purple dot-dashed contours, respectively

The plot for {min χ^2(wrong H) $-$ min χ^2(true H)} in the normal hierarchy case, Fig. 12, tells us that in the T2HK, the wrong mass hierarchy can still be favored if the true hierarchy is normal. In contrast, Fig. 15 shows that this is no longer the case if the true hierarchy is inverted.

The plots for $\Delta\delta_{CP}$, Figs. 13 and 16, show that the value of δ_{CP} that minimizes $\chi^2(\Pi)$ can deviate from the true δ_{CP} by more than 0.1 radian in the T2HK and more than 0.05 radian in the T2HKK, even with the alternative benchmark with the smaller non-unitary mixing. This augments our argument that the non-unitary mixing terms must be incorporated in the δ_{CP} measurement when a hint of non-unitarity has been discovered.
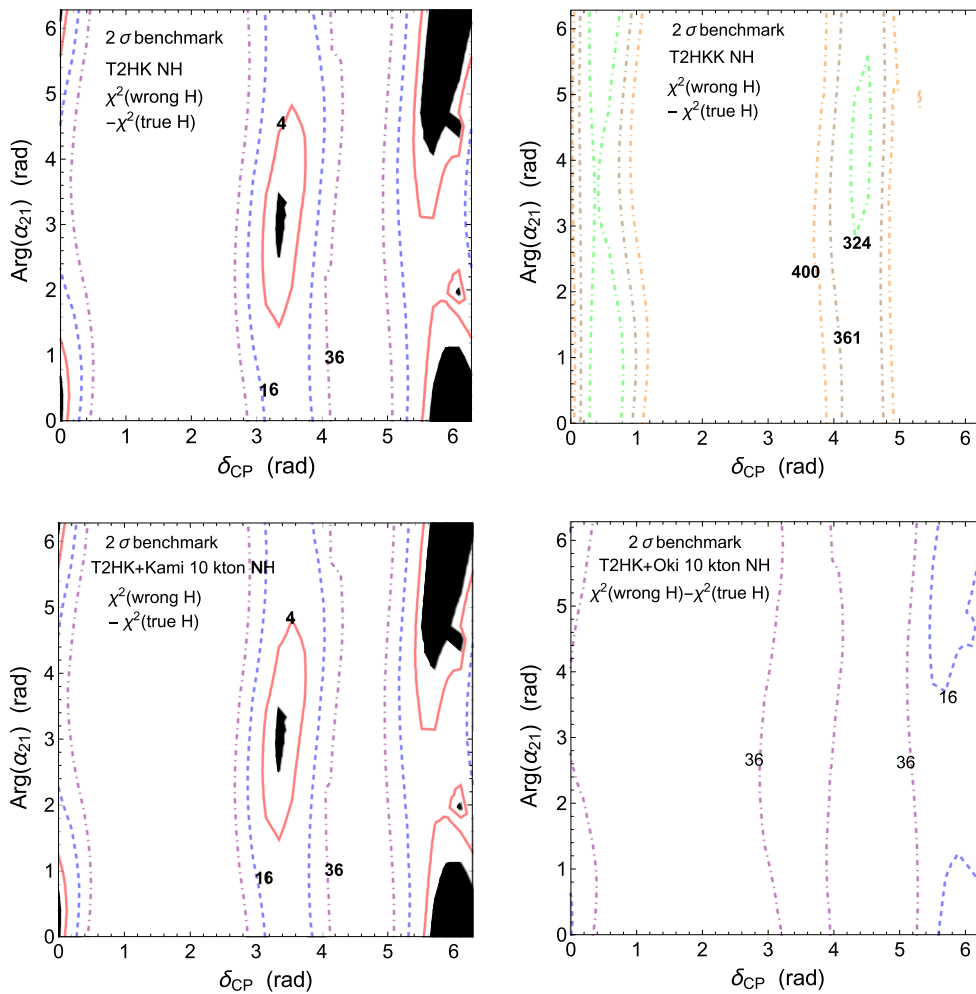
Fig. 12 The difference between the minima (with respect to δ_{CP} only) of $\chi^2(\Pi)$ for the wrong and true mass hierarchy, {min χ^2(wrong H) − min χ^2(true H)}. The benchmark with Eq. (37) is assumed, and the true mass hierarchy is normal. The upper-left, upper-right and lower-right subplots correspond to the T2HK, the T2HKK, and the plan of the T2HK plus a 10 kton water Cerenkov detector at Oki, respectively. For comparative study, we show in the lower-left a subplot

for a plan of the T2HK plus a 10 kton water Cerenkov detector at Kamioka. {min χ^2(wrong H) − min χ^2(true H)} = 4, 16, 36 on the red solid, blue dashed, and purple dot-dashed contours, respectively, and {min χ^2(wrong H) − min χ^2(true H)} = 18^2, 19^2, 20^2 on the green, brown, and orange dot-dashed contours, respectively. The black-filled regions are where the wrong mass hierarchy is favored over the true mass hierarchy, i.e., min χ^2(wrong H) − min χ^2(true H) < 0
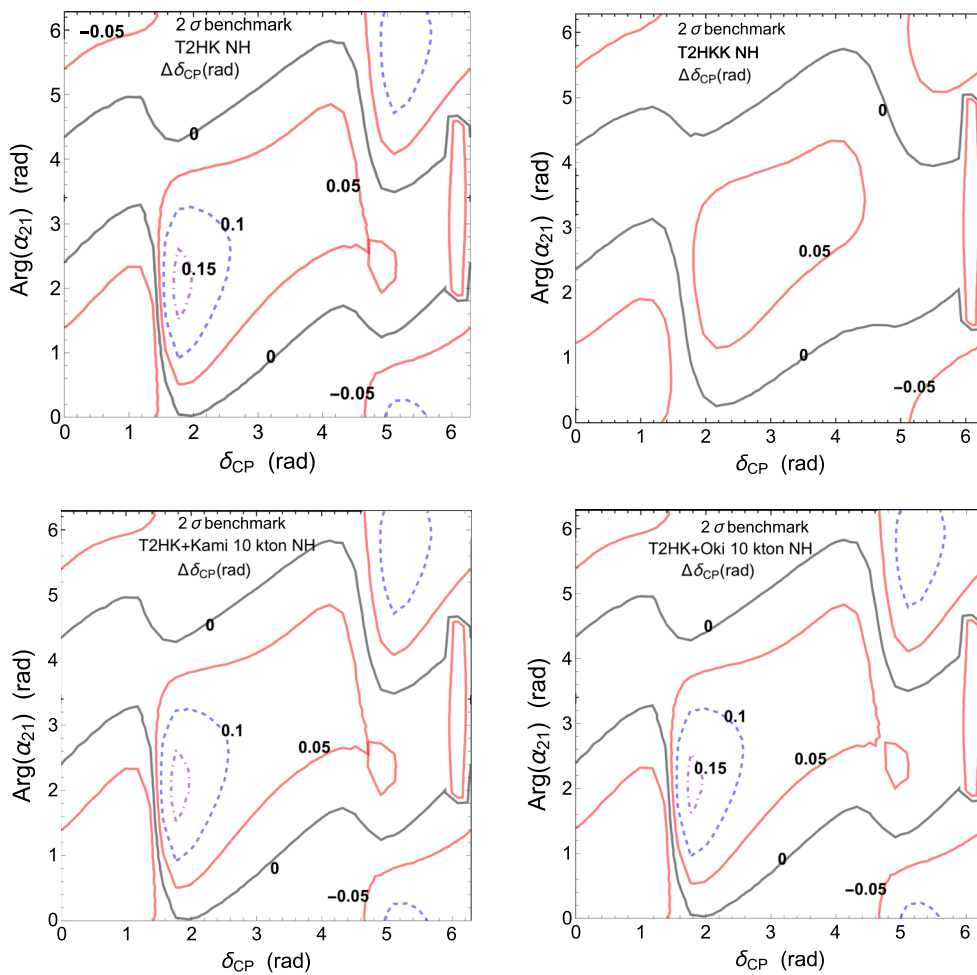
Fig. 13 The difference between the true value of δ_{CP}, and the value that minimizes $\chi^2(\Pi)$ of Eq. (32) with the true mass hierarchy. The benchmark with Eq. (37) is assumed, and the true mass hierarchy is normal. The upper-left, upper-right and lower-right subplots correspond to the T2HK, the T2HKK, and the plan of the T2HK plus a 10 kton water Cerenkov detector at Oki, respectively. For comparative study, we show in the lower-left a subplot for a plan of the T2HK plus a 10 kton water Cerenkov detector at Kamioka. $|\Delta\delta_{CP}| = 0$, 0.05rad, 0.1rad, and 0.15rad on the black solid, red sold, blue dashed, and purple dot-dashed contours, respectively
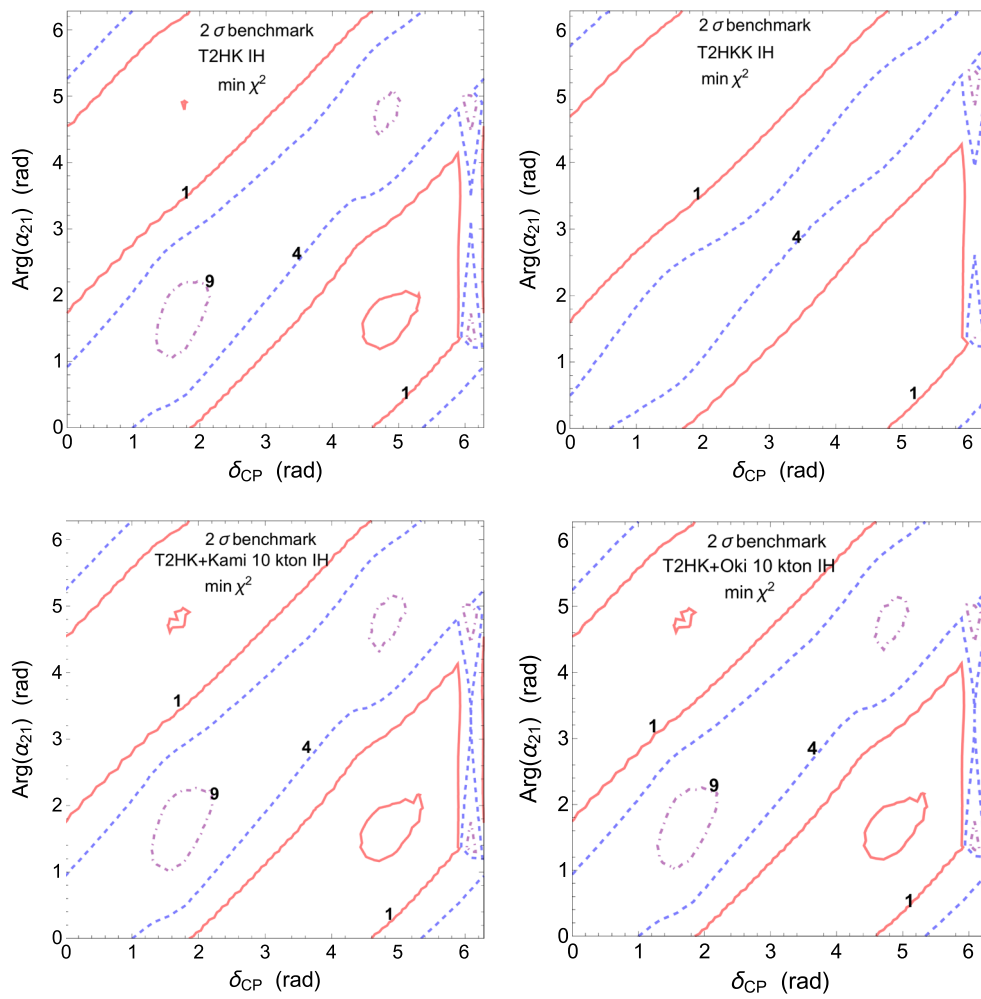
Fig. 14 The minimum of $\chi^2(\Pi)$ Eq. (32), min χ^2. The benchmark with Eq. (37) is assumed, and the true mass hierarchy is inverted. The upper-left, upper-right and lower-right subplots correspond to the T2HK, the T2HKK, and the plan of the T2HK plus a 10 kton water Cerenkov detector at Oki, respectively. For comparative study, we show in the lower-left a subplot for a plan of the T2HK plus a 10 kton water Cerenkov detector at Kamioka. min $\chi^2 = 1$, 4, 9 on the red solid, blue dashed, and purple dot-dashed contours, respectively
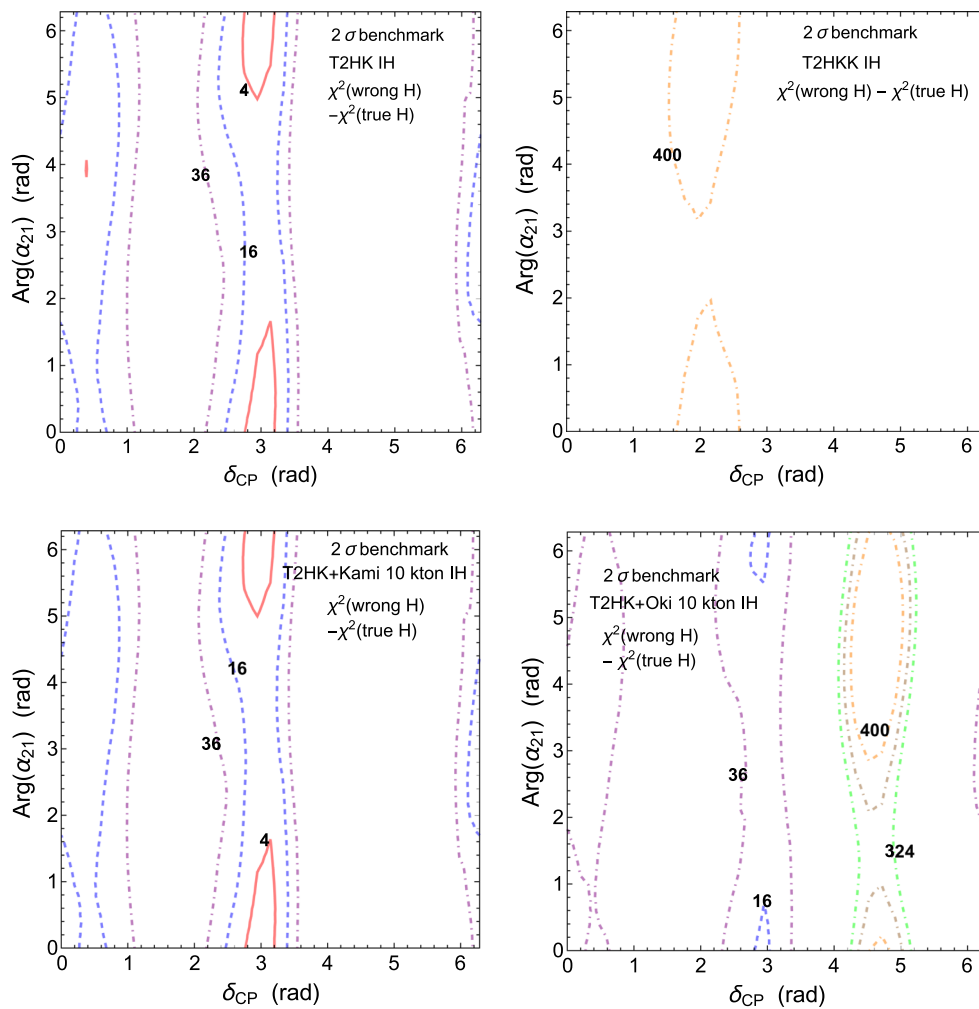
Fig. 15 The difference between the minima (with respect to δ_{CP} only) of $\chi^2(\Pi)$ for the wrong and true mass hierarchy, {min χ^2(wrong H) − min χ^2(true H)}. The benchmark with Eq. (37) is assumed, and the true mass hierarchy is inverted. The upper-left, upper-right and lower-right subplots correspond to the T2HK, the T2HKK, and the plan of the T2HK plus a 10 kton water Cerenkov detector at Oki, respec-

tively. For comparative study, we show in the lower-left a subplot for a plan of the T2HK plus a 10 kton water Cerenkov detector at Kamioka. {min χ^2(wrong H) − min χ^2(true H)} = 4, 16, 36 on the red solid, blue dashed, and purple dot-dashed contours, respectively, and {min χ^2(wrong H) − min χ^2(true H)} = 18^2, 19^2, 20^2 on the green, brown, and orange dot-dashed contours, respectively
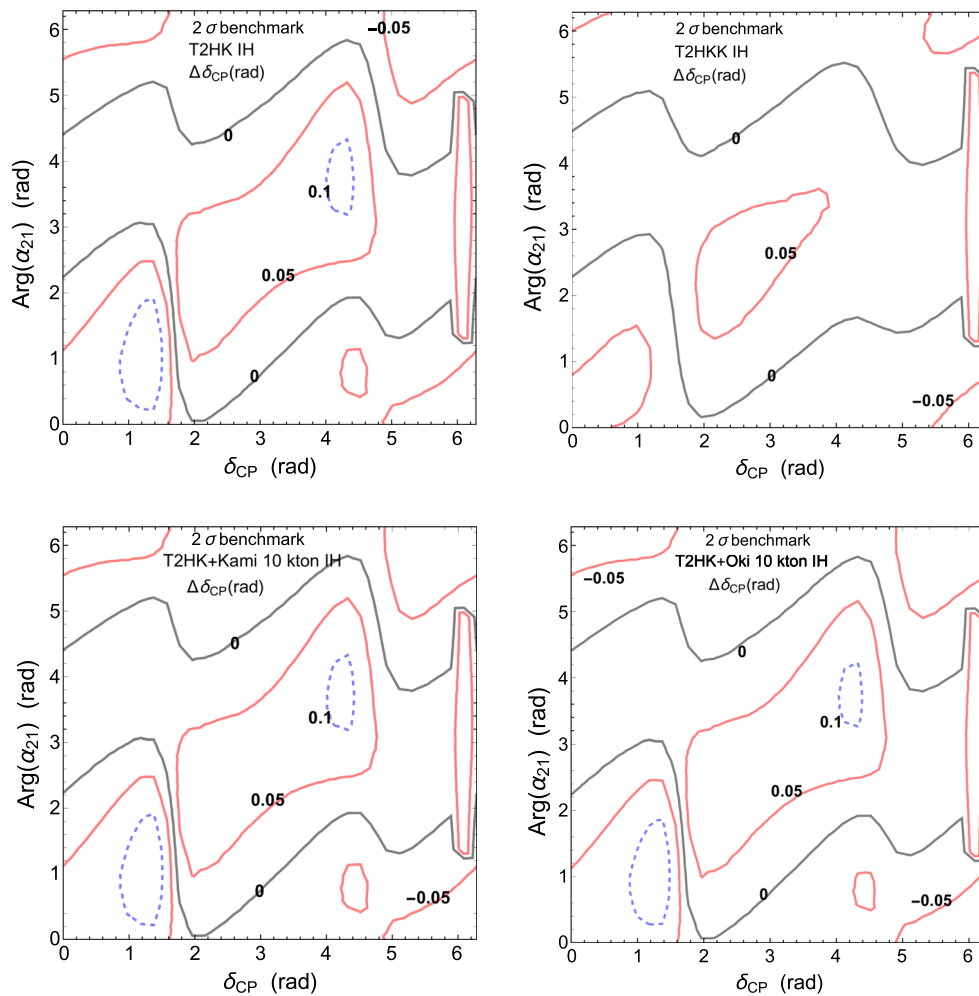
Fig. 16 The difference between the true value of δ_{CP}, and the value that minimizes $\chi^2(\Pi)$ of Eq. (32) $\Delta\delta_{CP}$ with the true mass hierarchy. The benchmark with Eq. (37) is assumed, and the true mass hierarchy is inverted. The upper-left, upper-right and lower-right subplots correspond to the T2HK, the T2HKK, and the plan of the T2HK plus a 10 kton water Cerenkov detector at Oki, respectively. For comparative study, we show in the lower-left a subplot for a plan of the T2HK plus a 10 kton water Cerenkov detector at Kamioka. $|\Delta\delta_{CP}| = 0$, 0.05rad, 0.1rad, and 0.15rad on the black solid, red sold, blue dashed, and purple dot-dashed contours, respectively

References

1. P. Minkowski, $\mu \rightarrow e\gamma$ at a rate of one out of 10^9 Muon decays? Phys. Lett. **67B**, 421 (1977)
2. T. Yanagida, Horizontal symmetry and masses of neutrinos. Conf. Proc. C **7902131**, 95 (1979)
3. S.L. Glashow, The future of elementary particle physics. NATO Sci. Ser. B **61**, 687 (1980)
4. R.N. Mohapatra, G. Senjanovic, Neutrino mass and spontaneous parity violation. Phys. Rev. Lett. **44**, 912 (1980)
5. J.A. Casas, A. Ibarra, Oscillating neutrinos and $\mu \rightarrow e, \gamma$. Nucl. Phys. B **618**, 171 (2001). arXiv:hep-ph/0103065
6. Z. Maki, M. Nakagawa, S. Sakata, Remarks on the unified model of elementary particles. Prog. Theor. Phys. **28**, 870 (1962)
7. B. Pontecorvo, Inverse beta processes and nonconservation of lepton charge. Sov. Phys. JETP **7**, 172 (1958)
8. B. Pontecorvo, Zh Eksp, Teor. Fiz. **34**, 247 (1957)
9. R.N. Mohapatra, Mechanism for understanding small neutrino mass in superstring theories. Phys. Rev. Lett. **56**, 561 (1986)
10. R.N. Mohapatra, J.W.F. Valle, Neutrino mass and Baryon number nonconservation in superstring models. Phys. Rev. D **34**, 1642 (1986)
11. K. Abe et al., [Hyper-Kamiokande Proto- Collaboration], Physics potential of a long-baseline neutrino oscillation experiment using a J-PARC neutrino beam and hyper-Kamiokande. PTEP **2015**, 053C02 (2015). arXiv:1502.05199 [hep-ex]
12. K. Abe et al., [Hyper-Kamiokande proto- Collaboration], Physics potentials with the second hyper-Kamiokande detector in Korea. arXiv:1611.06118 [hep-ex]
13. K. Hagiwara, Physics prospects of future neutrino oscillation experiments in Asia. Nucl. Phys. Proc. Suppl. **137**, 84 (2004). arXiv:hep-ph/0410229
14. M. Ishitsuka, T. Kajita, H. Minakata, H. Nunokawa, Resolving neutrino mass hierarchy and CP degeneracy by two identical detectors with different baselines. Phys. Rev. D **72**, 033003 (2005). arXiv:hep-ph/0504026
15. K. Hagiwara, N. Okamura, K.I. Senda, Solving the neutrino parameter degeneracy by measuring the T2K off-axis beam in Korea.

Phys. Lett. B **637**, 266 (2006). (Erratum: [Phys. Lett. B **641**, 491 (2006)]). arXiv:hep-ph/0504061

16. K. Hagiwara, N. Okamura, K.I. Senda, Physics potential of T2KK: an extension of the T2K neutrino oscillation experiment with a far detector in Korea. Phys. Rev. D **76**, 093002 (2007). arXiv:hep-ph/0607255

17. T. Kajita, H. Minakata, S. Nakayama, H. Nunokawa, Resolving eight-fold neutrino parameter degeneracy by two identical detectors with different baselines. Phys. Rev. D **75**, 013006 (2007). arXiv:hep-ph/0609286

18. K. Hagiwara, N. Okamura, Solving the degeneracy of the lepton-flavor mixing angle theta(ATM) by the T2KK two detector neutrino oscillation experiment. JHEP **0801**, 022 (2008). arXiv:hep-ph/0611058

19. P. Huber, M. Mezzetto, T. Schwetz, On the impact of systematical uncertainties for the CP violation measurement in superbeam experiments. JHEP **0803**, 021 (2008). arXiv:0711.2950 [hep-ph]

20. K. Hagiwara, N. Okamura, Re-evaluation of the T2KK physics potential with simulations including backgrounds. JHEP **0907**, 031 (2009). arXiv:0901.1517 [hep-ph]

21. F. Dufour, T. Kajita, E. Kearns, K. Okumura, Further study of neutrino oscillation with two detectors in Kamioka and Korea. Phys. Rev. D **81**, 093001 (2010). arXiv:1001.5165 [hep-ph]

22. T. Kiwanami, N. Okamura, K.i Senda, Physics potential of neutrino oscillation experiment with a far detector in Oki Island along the T2K baseline. JHEP **1306**, 036 (2013). arXiv:1209.2763 [hep-ph]

23. K. Hagiwara, P. Ko, N. Okamura, Y. Takaesu, Revisiting T2KK and T2KO physics potential and $\nu_\mu - \bar{\nu}_\mu$ beam ratio. Eur. Phys. J. C **77**(3), 138 (2017). arXiv:1605.02368 [hep-ph]

24. A. Badertscher, T. Hasegawa, T. Kobayashi, A. Marchionni, A. Meregaglia, T. Maruyama, K. Nishikawa, A. Rubbia, A possible future long baseline neutrino and nucleon decay experiment with a 100 kton liquid argon TPC at Okinoshima using the J-PARC neutrino facility. arXiv:0804.2111 [hep-ph]

25. O.G. Miranda, M. Tortola, J.W.F. Valle, New ambiguity in probing CP violation in neutrino oscillations. Phys. Rev. Lett. **117**(6), 061804 (2016). arXiv:1604.05690 [hep-ph]

26. S.F. Ge, P. Pasquini, M. Tortola, J.W.F. Valle, Measuring the leptonic CP phase in neutrino oscillations with nonunitary mixing. Phys. Rev. D **95**(3), 033005 (2017). arXiv:1605.01670 [hep-ph]

27. D. Dutta, P. Ghoshal, Probing CP violation with T2K, NOνA and DUNE in the presence of non-unitarity. JHEP **1609**, 110 (2016). arXiv:1607.02500 [hep-ph]

28. D. Dutta, P. Ghoshal, S. Roy, Effect of non unitarity on neutrino mass hierarchy determination at DUNE, NOνA and T2K. Nucl. Phys. B **920**, 385 (2017). arXiv:1609.07094 [hep-ph]

29. F.J. Escrihuela, D.V. Forero, O.G. Miranda, M. Tortola, J.W.F. Valle, arXiv:1612.07377 [hep-ph]

30. F.J. Escrihuela, D.V. Forero, O.G. Miranda, M. Tortola, J.W.F. Valle, On the description of nonunitary neutrino mixing. Phys. Rev. D **92**(5), 053009 (2015). (Erratum: [Phys. Rev. D **93**(11), 119905 (2016)]). arXiv:1503.08879 [hep-ph]

31. K. Abe et al., [T2K Collaboration], The T2K experiment. Nucl. Instrum. Meth. A **659**, 106 (2011). arXiv:1106.1238 [physics.ins-det]

32. K. Hagiwara, N. Okamura, K.I Senda, The earth matter effects in neutrino oscillation experiments from Tokai to Kamioka and Korea. JHEP **1109**, 082 (2011). arXiv:1107.5857 [hep-ph]

33. J. Schechter, J.W.F. Valle, Neutrino masses in SU(2) × U(1) theories. Phys. Rev. D **22**, 2227 (1980)

34. Z.Z. Xing, Correlation between the charged current interactions of light and heavy Majorana neutrinos. Phys. Lett. B **660**, 515 (2008). arXiv:0709.2220 [hep-ph]

35. Z.Z. Xing, A full parametrization of the 6 × 6 flavor mixing matrix in the presence of three light or heavy sterile neutrinos. Phys. Rev. D **85**, 013008 (2012). arXiv:1110.0083 [hep-ph]

36. G. Czapek et al., Branching ratio for the rare pion decay into positron and neutrino. Phys. Rev. Lett. **70**, 17 (1993)

37. E. Nardi, E. Roulet, D. Tommasini, Limits on neutrino mixing with new heavy particles. Phys. Lett. B **327**, 319 (1994). arXiv:hep-ph/9402224

38. A. Abada, D. Das, A.M. Teixeira, A. Vicente, C. Weiland, Tree-level lepton universality violation in the presence of sterile neutrinos: impact for R_K and R_π. JHEP **1302**, 048 (2013). arXiv:1211.3052 [hep-ph]

39. C. Patrignani et al., [Particle Data Group], Review of particle physics. Chin. Phys. C **40**(10), 100001 (2016)

40. A. Bazavov et al., Kaon semileptonic vector form factor and determination of $|V_{us}|$ using staggered fermions. Phys. Rev. D **87**, 073012 (2013). arXiv:1212.4993 [hep-lat]

41. P.A. Boyle et al., [RBC/UKQCD Collaboration], The kaon semileptonic form factor in $N_f = 2 + 1$ domain wall lattice QCD with physical light quark masses. JHEP **1506**, 164 (2015). arXiv:1504.01692 [hep-lat]

42. S. Antusch, O. Fischer, Non-unitarity of the leptonic mixing matrix: present bounds and future sensitivities. JHEP **1410**, 094 (2014). arXiv:1407.6607 [hep-ph]

43. E. Fernandez-Martinez, J. Hernandez-Garcia, J. Lopez-Pavon, Global constraints on heavy neutrino mixing. JHEP **1608**, 033 (2016). arXiv:1605.08774 [hep-ph]

44. M. Blennow, P. Coloma, E. Fernandez-Martinez, J. Hernandez-Garcia, J. Lopez-Pavon, Non-unitarity, sterile neutrinos, and non-standard neutrino interactions. JHEP **1704**, 153 (2017). arXiv:1609.08637 [hep-ph]

45. P. Astier et al., [NOMAD Collaboration], Search for nu(mu) - > nu(e) oscillations in the NOMAD experiment. Phys. Lett. B **570**, 19 (2003). arXiv:hep-ex/0306037

46. J. Arafune, M. Koike, J. Sato, CP violation and matter effect in long baseline neutrino oscillation experiments. Phys. Rev. D **56**, 3093 (1997). (Erratum: [Phys. Rev. D **60**, 119905 (1999)]). arXiv:hep-ph/9703351

47. http://www.t2k.org/docs/talk/254/lmagalet. Accessed 1 Apr 2017

48. R.A. Smith, E.J. Moniz, Neutrino reactions on nuclear targets. Nucl. Phys. B **43**, 605 (1972). (Erratum: [Nucl. Phys. B **101**, 547 (1975)])